Bulletin of the Mineral Research and Exploration

http://bulletin.mta.gov.tr

Stratigraphy of the metamorphic rocks of Niğde Massif and new evidence of Triassic rifting of the Inner Tauride Ocean (Central Anatolia, Türkiye)

Mustafa Kemal ÖZKAN[a*], Metin BEYAZPİRİNÇ[b], Ali Ekber AKÇAY[b], Muhamed ÇOBAN[c], Osman CANDAN[d], Osman Ersin KORALAY[d], Meftun Kerem SÖNMEZ[b] and Halil YUSUFOĞLU[b]

[a]*General Directorate of Mineral Research and Exploration, Eastern Black Sea Regional Directorate, Trabzon, Türkiye*
[b]*General Directorate of Mineral Research and Exploration, Depoartment of Geological Researches, Ankara, Türkiye*
[c]*General Directorate of Mineral Research and Exploration, Southeastern Anatolia Regional Directorate, Diyarbakır, Türkiye*
[d]*Dokuz Eylül University, Geological Engineering Department, İzmir, Türkiye*

Research Article

Keywords:
Niğde Massif Metamorphics, Stratigraphy, Triassic Rifting, Inner Tauride Ocean.

ABSTRACT

Metamorphites of Niğde Massif, which form the basis of study area covering the Niğde vicinity in Central Anatolia, are composed of Late Devonian Gümüşler, Carboniferous-early Permian Kaleboynu late Permian Kızıldağ formation and unconformable Triassic-Late Cretaceous cover units from bottom to the top, which are separated from each other with unconformities. The Triassic succession (Söğütlüdere formation) of phyllite-marble-schist alternations with common amphibolite levels is first distinguished in this study, unconformably overlies the Paleozoic succession. Thick homogeneous marbles of Jurassic-Cretaceous period, is defined by quartzite at the bottom representing the unconformity at the base, is defined as the Kırtepe formation. The succession probably ends with the Late Cretaceous metaflysch (Kırkpınar formation) constituting metaophiolite blocks with unconformable contact relationships. Amphibolite sample of the Söğütlüdere formation gives 239 Ma (Middle Triassic) age, which is interpreted as the crystallization age of the primary basic magmatism. The youngest detrital zircon ages (223-224 Ma) obtained from the metaclastics of the same formation shows that the primary deposition age of the formation is probably Late Triassic, which is consistent with this data. Geochemical data indicate an extensional environment of the alkaline composition and anorogenic originated basic volcanism developed on the continental crust. When these results evaluated together with the regional data, the metabasites of the Söğütlüdere formation can be interpreted as the first phase products of rifting, which commenced with the rifting process of the Tauride-Anatolide Platform in the Triassic period and resulted in the opening of the Inner Tauride Ocean and the break off the Kırşehir Block.

Received Date: 19.08.2021
Accepted Date: 31.01.2022

1. Introduction

The study area located on the Kırşehir Block in Central Anatolia (Şengör and Yılmaz, 1981; Okay and Tüysüz, 1999) covers the Niğde vicinity. The area bounded by the İzmir-Ankara-Erzincan Suture Zone (North Anatolian Ophiolite Belt) in the north and the Inner Tauride Suture in the south form the Kırşehir Block, one of the main tectonic units of Türkiye. Tuz Gölü and Central Anatolian faults predominantly follow these suture zones (Figure 1). Kırşehir Block generally consists of ophiolites and nappes of oceanic origin emplaced on high grade metamorphic rocks and

Citation Info: Özkan, M. K., Beyazpirinç, M., Akçay, A. E., Çoban, M., Candan, O., Koralay, O. E., Sönmez, M. K., Yusufoğlu, H. 2023. Stratigraphy of the Niğde Massif metamorphics and strong evidence of Triassic rifting of the inner Tauride Ocean (Central Anatolia, Türkiye). Bulletin of the Mineral Research and Exploration 170, 57-85. https://doi.org/10.19111/bulletinofmre.1133242

**Corresponding author: Mustafa Kemal ÖZKAN, kemal.ozkan@mta.gov.tr*

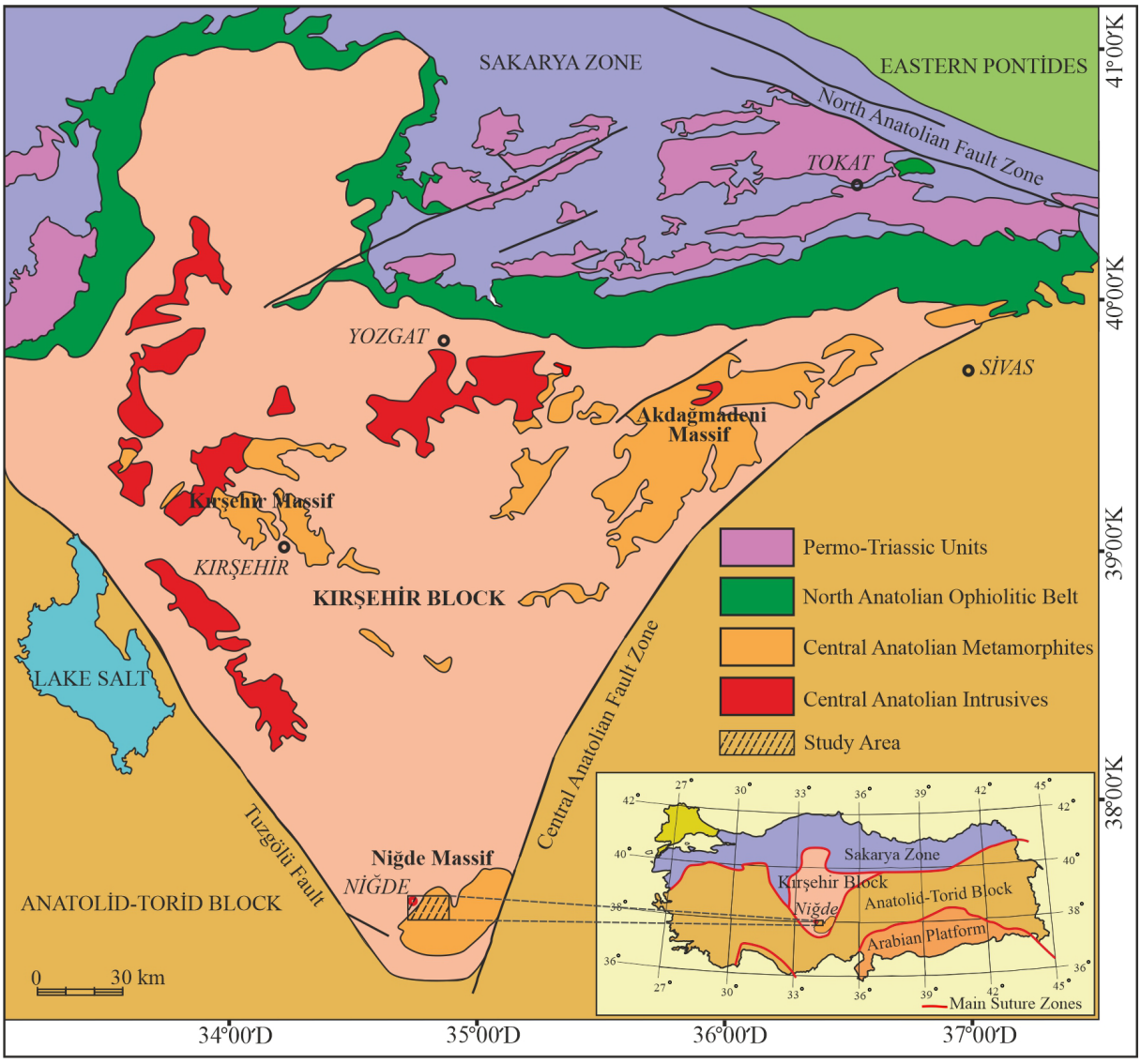

Figure 1- Location map of the study area.

granitic plutons together with their surface equivalents cutting cross those. All these units are covered by Paleogene and Neogene sedimentary rocks. The Niğde Massif has been the subject of detailed research for many years, but the ages and stratigraphies of the rocks that make up the massif remain debated. In this study, the main aim is to reveal the lithofacies features and contact relationships of the above-mentioned rocks with a regional research, to determine their age with paleontological-radiometric data, and to discuss the evolution of the massif using the results.

Detailed studies on the stratigraphy of the Niğde Massif were made by Göncüoğlu (1977, 1981). It was stated that Gümüşler formation, Kaleboynu formation and Aşıgediği formation, from bottom to top, is grouped under Niğde group and they are in cutting-cross relationship with Üçkapılı granodiorite. In addition, it was argued that the metamorphism evolved from medium pressure-high temperature type to low pressure-high temperature type and PT conditions reached partial melting occassionally, and the main metamorphism phase and ophiolite emplacement in the massif took place before the Cenomanian. Yalınız and Göncüoğlu (1998) stated that the ophiolites on the Central Anatolian metamorphic rocks, despite being disturbed, preserved their primary ophiolitic sequence and they were cut-cross by granitoids. They argued

that the ophiolites developed in the fore-arc basin due to an intraoceanic subduction in the İzmir-Ankara Ocean during the middle Turonian-early Santonian, and were emplaced onto the Central Anatolian metamorphic rocks following the early Santonian and prior to the Maastrichtian. Aydın et al. (1998) studied the Uppermost Late Cretaceous magmatism in the Central Anatolian Crystalline Complex. Whitney et al. (2001) suggested that the Central Anatolian Crystalline Complex can be divided into at least four tectonic blocks (Kırşehir, Akdağ, Niğde and Aksaray massifs) indicating different temperature-pressure-time evolutions. They stated that the massifs were exposed to thrust and folding processes due to the collision in the north, and they slowly exhumed with following erosion. Whitney et al. (2007) studied the Yo-yo tectonics during the strike-slip faulting of the Niğde Massif. They stated that two complete burial/exhumation cycles were present through the Massif in an oblique-slip deformation zone over a period longer than ~80 Ma, one observed at a regional scale and the other at a more local scale from the Cretaceous (burial) to Miocene (cooling and exhumation). Boztuğ et al. (2009) argued that Central Anatolian granitoid melts emerged after the collision, an oceanic arc emplaced on the Tauride-Anatolide platform during Campanian-Maastrichtian and rapidly uplifting in the early-middle Paleocene resulted. Advokaat et al. (2014) mentioned block rotations in Paleocene. Cengiz Çinku et al. (2016) concluded that the Niğde-Kırşehir Massif rotated counterclockwise up to 25.5°±7.3° during the Middle Eocene in their paleomagnetism study. Demircioğlu and Eren (2003, 2017) determined that both the Niğde Massif and Paleocene-Eocene cover rocks were deformed together, based on mesoscopic tectonic analyses. They stated that the metamorphics forming the Niğde Massif underwent ductile deformation with at least four phases (D_1, D_2, D_3 and D_4). Çoban (2019) stated that the rocks of the Niğde Massif underwent multi-phase deformation and high-grade metamorphism and acquired a foliated structure before the Late Cretaceous. Due to closure of the Inner Tauride Ocean, Ulukışla group and rocks of the massif were together exposed before the Oligocene and they stated strike-slip and normal faults developed in the region during the neotectonic period. Demircioğlu and Coşkuner (2021) argued that type-3 fold interference structures, especially branching to the northeast and southwest, developed in the rocks as a result of multi-stage deformation of high-grade metamorphic rocks of the Niğde Massif.

In this study, the stratigraphic characteristics of the metamorphic masses of the Niğde Massif were revealed in detail using the new stratigraphic, sedimentological, petrographic, geochemical and geochronological data obtained within the scope of the project as well as the previous studies. Additionally, the meaning and importance of the Triassic succession, which is distinguished for the first time in this study, including the first phase products of the Inner Tauride Ocean rifting are discussed in terms of the regional geology.

2. Regional Geology

The metamorphic, magmatic and ophiolitic rock assemblages in Central Anatolia were named as Central Anatolian Crystalline Complex (CACC) (Göncüoğlu et al., 1991, 1993). Considering the geographical areas where the metamorphic masses outcrop in the CACC were defined with different names; Akdağ Massif (Baykal, 1947), Kırşehir Crystalline Massif (Bailey and McCallien, 1950; Egeran and Lahn, 1951), Central Anatolia Massif, Kızılırmak Massif (Ketin, 1955, 1963; Erkan and Ataman, 1981), Niğde group/Niğde Massif (Göncüoğlu, 1977, 1981), Kaman group (Seymen, 1981*a, b*) and Central Anatolian Crystalline Complex (Erler and Bayhan, 1995).

The rocks of İzmir-Ankara-Erzincan Zone (North Anatolian Ophiolite Belt) and Sakarya Zone (Permo-Triassic units) outcrop in the north of the Kırşehir Block whereas Inner Tauride Suture Belt and Anatolide-Tauride Block rocks in the westerly-southerly and easterly (Figure 1). Sakarya Zone, İzmir-Ankara-Erzincan Zone, Kırşehir Massif, Inner Tauride Suture Belt and Anatolide-Tauride Block units are observed in tectonic relationship (nappe) with each other from north to south. The Niğde Massif units in Kırşehir Block, which will be explained in detail in this study, consitute the basement. Salt Lake Basin units represented by deep sea sediments consisting of the remains of the Inner Tauride Ocean are observed in the western part of the Kırşehir Block whereas the presence of the basin and post-collisional basin

sediments of the Inner Tauride Ocean is observed in the southern part. Görür et al. (1998) suggested that Ulukışla Basin developed as a fore-arc basin due to subduction of the Inner Tauride Ocean between Bolkar carbonate platform and Kırşehir-Niğde microplates towards northerly direction. On the other hand, some researchers argued that this basin developed resulting with the extensional (Göncüoğlu et al., 1991; Çemen et al., 1999) or transtensional tectonic regime (Alpaslan et al., 2006) due to collision within Anatolide-Tauride platform following the closure of the Neotethys Ocean. Clark and Robertson (2002) stated that Ulukışla Basin is a basin that developed under the effect of extensional tectonics on the Inner Tauride Suture Zone. In the south of the Inner Tauride Suture Belt separating the Kırşehir Block and the Tauride-Anatolide Block, the Tavşanlı Zone and Afyon Zone units of the Tauride-Anatolide Block crop out with tectonic contacts. The units of the Kırşehir Block and the Anatolide-Tauride Block are bounded by the Tuzgölü Fault towards west and by the Central Anatolian Fault Zone (Ecemiş Fault Zone) towards easterly direction. In the study area covering the Niğde Massif, metamorphic rocks, ophiolitic rocks, granitoid and cover units of the Ulukışla Basin and Ürgüp Basin crop out in the most general sense (Figure 2).

3. Material and Methods

Detailed geologial mapping was conducted in the study area between Niğde and Çamardı (1/100000 in scale, Adana-M33 sheet) and correlations together with observations were also made out of the study area if needed. Thin sections of the samples collected from the study area were prepared and examined in detail under the polarizing microscope and their petrographic properties were defined. Chemical analyzes (major, trace and rare earth element) of selected 12 samples using field observations and petrographic examinations were carried out at Department of Mineral Analysis and Technology Laboratories of General Directorate of Mineral Research and Exploration (MTA). The samples were first grounded into powders in the laboratory. The powdered sample (0.2 g) was mixed with 1.5 g of $LiBO_2$ and dried at 105°C, and major oxide analyzes were performed in a Thermo-ARL brand XRF device. The samples were solved according to TS ISO 14869-1 and TS ISO 14869-2 and analyzed in ICP-OES and ICP-MS devices. Zircon U/Pb dating of two samples from the metabasite member of the Söğütlüdere formation was conducted at the University of Arizona, Department of Geosciences Laboratory (USA). After the rock samples had gone through standard mineral separation processes, the zircons were hand-picked in alcohol and placed in epoxy with reference materials. The discs containing the grains were then wet abraded with sandpaper of various thicknesses and polished with diamond paste. Followingly, cathodoluminescence (CL) images were captured on a Philips XL-30 scanning electron microscope (SEM) equipped with the Bruker Quanta 200 energy dispersion X-ray microanalysis system at the Electron Microbeam/X-Ray Diffraction Laboratory (EMXDF), University of British Columbia. An operating voltage of 15 kV with a spot diameter of 6 μm and a peak count time of 30 seconds was used. After removal of the carbon coating, the grain holding surface was washed with mild soap and rinsed with high purity water. Prior to analysis, the disc surface was cleaned with 3 N HNO_3 acid and rinsed again with high-purity water to remove any superficial Pb contamination that might interfere with the early part of spot analyses.

4. Stratigraphy of the Metamorphic Rocks of Niğde Massif

The metamorphic rocks of the Niğde Massif, which form the basis of the study area and can be correlated with the Yahyalı nappe (Blumenthal, 1952) located in the Taurus Mountains in terms of stratigraphic characteristics, constitute conformable and transitional contacts of the Late Devonian Gümüşler, Carboniferous-early Permian Kaleboynu, late Permian Kızıldağ formation unconformably overlying the Triassic Söğütlüdere formation which is first distinguished and defined, Jurassic-Cretaceous Kırtepe and Late Cretaceous Kırkpınar formations from the bottom to the top. The Late Devonian-Early Cretaceous sequence has undergone metamorphism under amphibolite and above facies progradely and occasionally greenschist facies retrogradely. The metamorphics of the Niğde Massif, from bottom to top, consist of quartzite, quartz schist, mica schist, calc schist, occasionally plaque-like marble, dolomitic marble, metabasite, talc schist, metasiltstone, metamudstone, cherty marble and schist, marble and

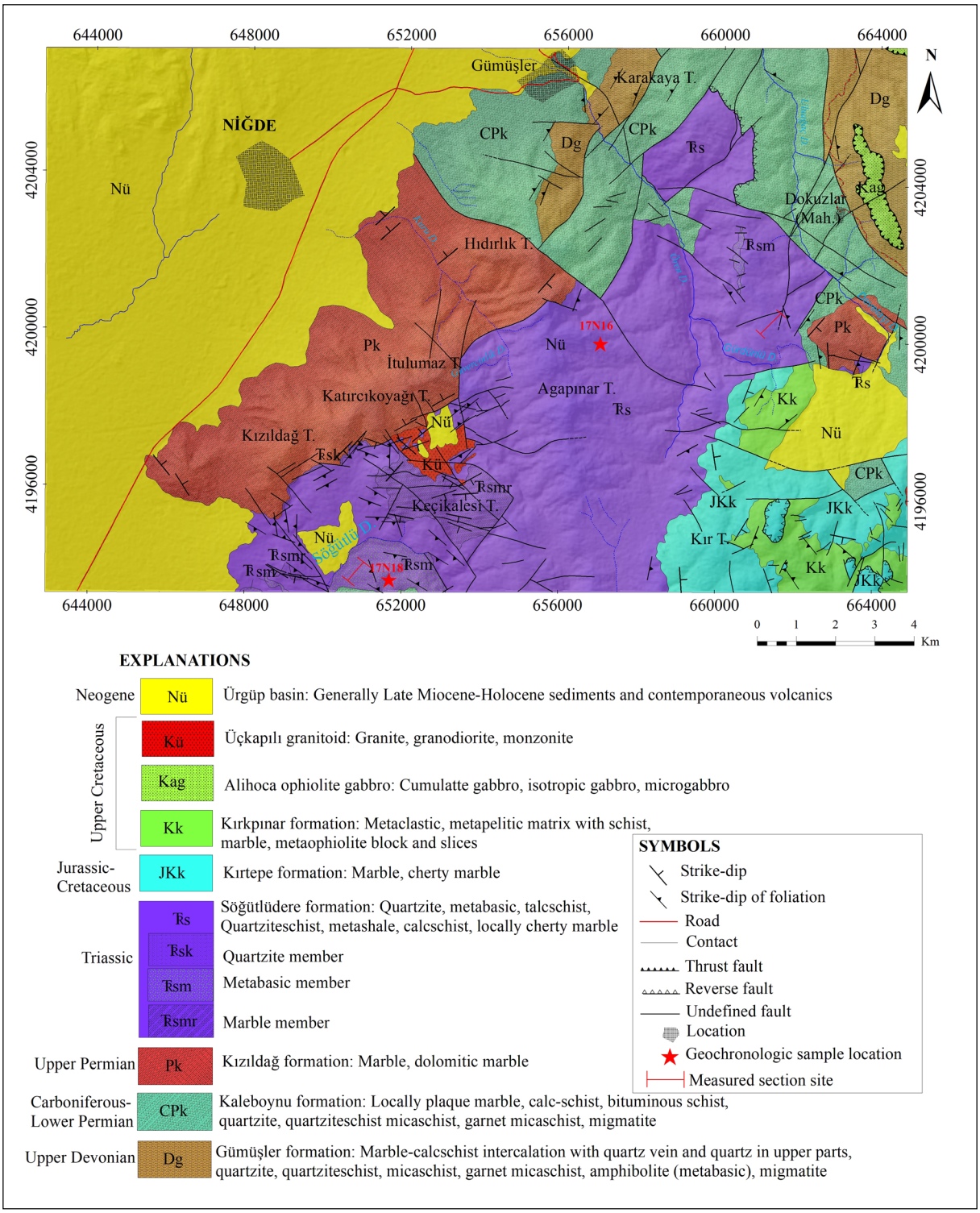

Figure 2- Geological map of the study area.

metaophiolite blocks in a metaclastic-metapelitic matrix (Figure 3).

The Gümüşler formation, located at the base of the Niğde Massif and named by Göncüoğlu (1981), is generally greenish, gray in color, with partially migmatized sillimanite-garnet mica schist at lower sections, paragneiss, amphibolite, quartz schist, quartzite, and amphibolite intercalations in the upper

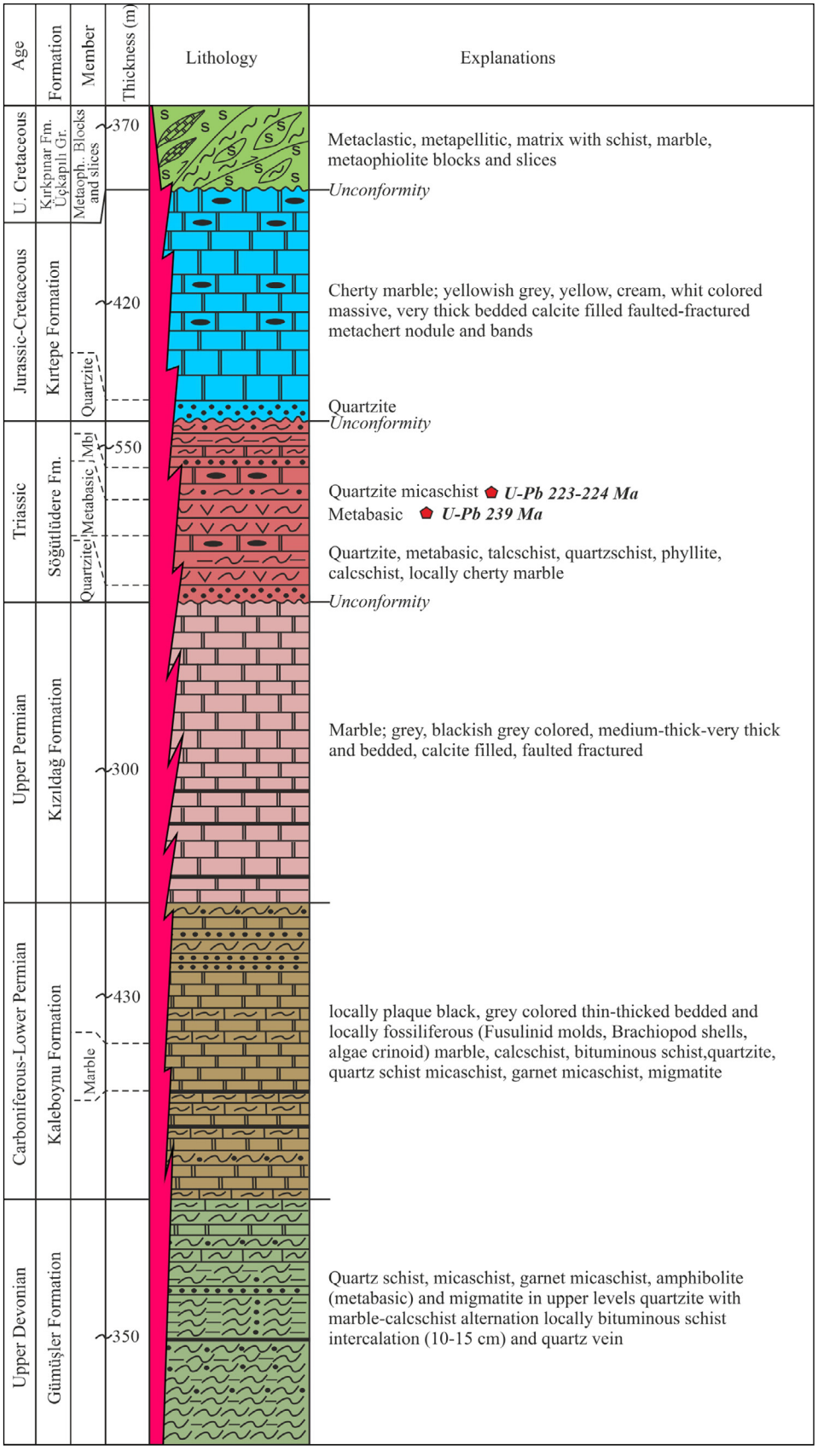

Figure 3- Generalized columnar section of the Niğde Massif.

parts within the calcschist-marble levels (Figure 4). Considering its stratigraphic position and correlating it with similar facies in the Taurus Mountains (Late Devonian successions in the Geyikdağı unit and Aladağ nappe and their metamorphic equivalents in the Bolkardağı Nappe and Yahyalı Nappe), age of the unit was determined as Late Devonian. The unit can be correlated with Yahyasaray formation located at the base of the Akdağmadeni Massif (Beyazpirinç and Akçay, 2017), metapelites in the Akdağmadeni metasedimentary group (Şahin, 1991), a part of Köklüdere formation (Dökmeci, 1980) in the Akdağ metamorphic group and Kalkanlıdağ formation (Seymen, 1982) at the base of Kırşehir Massif.

The Kaleboynu formation, named by Göncüoğlu (1981), is generally yellowish gray in color and consists of calcschist, plaque marble-dolomitic marble, quartzite, quartz schist, mica schist, sericite-schist, with occasionally marble lenses and bituminous schist intercalations (Figure 5). Hornfels and calc-silicate fels rocks were occasionally developed depending on the granite intrusions. The Kızıldağ formation conformably overlies the Kaleboynu formation, which overlies the Gümüşler formation conformably and transitionally, and the Söğütlüdere formation unconformably. Fusulinid molds, brachiopoda and macrofossil shell fragments were observed in the unit, and Carboniferous-early Permian age has been suggested considering their correlation with similar facies in the Taurus Mountains (Carboniferous-early Permian successions in the Geyikdağı unit and Carboniferous-early Permian sequences in the Aladağ nappe and their metamorphic equivalents in the Bolkardağı nappe and Yahyalı nappe) for the Kaleboynu formation. The unit can be correlated with Akçakışla formation (Beyazpirinç and Akçay, 2017) in Akdağmadeni Massif, semimetapelites (Şahin, 1991) in Akdağmadeni metasedimentery group, parts of the Köklüdere and Özerözü formations (Dökmeci, 1980), Tamadağ formation (Seymen, 1981*b*) defined around Kaman district (Kırşehir province) and Kervansaray formation (Kara and Dönmez, 1990) in Kırşehir Massif.

Figure 4- a) Schist-calcschist-marble alternation in the upper levels of the Gümüşler formation, b) metabasites cutting-cross quartz mica schists and c) migmatized metapelites.

Figure 5- a) Schist-calcschist-marble intercalation containing bituminous schist intercalations in the Kaleboynu formation, b) brachiopodas and c) marbles containing fusulinid molds.

The Kızıldağ formation, which is equivalent of a part of the Aşıgediği formation (Göncüoğlu, 1981) and was distinguished for the first time in this study, is gray, blackish gray in color, thin-thick bedded, medium-coarse crystalline and joint systems have commonly developed. Dissolution voids are observable. It consists of marble levels occasionally intercalated with bituminous schist and dolomitic marble. Considering its stratigraphic position and correlating with similar facies in the Taurus Mountains, late Permian age has been suggested for the unit, which conformably overlies the Kaleboynu formation. The unit can be correlated with Topaktaş formation in Akdağmadeni Massif (Beyazpirinç and Akçay, 2017), metacarbonates in Akdağmadeni metasedimentary group (Şahin, 1991) and Bozçaldağ formation in Kırşehir Massif (Seymen, 1982). Triassic Söğütlüdere, Jurassic-Cretaceous Kırtepe and Late Cretaceous Kırkpınar formations, which overlie all these Paleozoic successions and are unconformably separated from each other, were distinguished for the first time in this study. Kırtepe formation, with quartzite units reaching up to 50 m in thickness and defining the unconformable contact relation at the base, is composed of occasionally dolomitized homogenous marble. General characteristics of the formation are that weathering colour is gray and fresh surface is in different colours i.e. yellow, cream, gray and white. It is thick-bedded and massive in texture, and joint-fracture systems are also present. Jurassic-Cretaceous age was suggested considering the stratigraphic position of the unit, which unconformably overlies the Gümüşler formation, Kervansaray formation and Söğütlüdere formation, and correlations with similar facies in the Taurus Mountains. The unit can be correlated with a part of the Saytepe formation in the Kırşehir Massif (Beyazpirinç et al., 2020), the Hisarbey formation in the Akdağmadeni Massif (Beyazpirinç and Akçay, 2017) and the Aşıgediği formation in the Niğde Massif (Göncüoğlu, 1981).

Kırkpınar formation, which is the upper-most part of the Niğde Massif and is distinguished for the first time in this study, generally presents the Late Cretaceous blocky metaflysch characteristics consisting of quartzite, quartz schist, mica schist and metabasite with metaophiolite, marble, schist blocks and rarely observed metaconglomerate (channel fillings) (Figure 6). The unit can be considered as the metamorphic equivalent of the Cenomanian Karaböğürtlen formation in the Western Taurus Mountains, which is first named by Philippson (1915) and it can be correlated with Davulbaz formation in Akdağmadeni Massif (Beyazpirinç and Akçay, 2017) and partly correlated with blocky levels of Özerözü formation (Dökmeci, 1980) in Akdağ metamorphic group.

Triassic metamorphics in the study area constituting the main subject of this study is distinguished for the first time in this study and named as Söğütlüdere formation. Quartzite, quartz-schist and sericite-schists at the base of the Söğütlüdere formation is distinguished as Quartzite member. Amphibolite/metabasites with marble intercalations are defined as Metabasite member. Thick marble levels as interbeds and lenses are defined as Marble member. The unit generally starts with a quartzite unconformity and is represented by quartz mica schist, mottled coloured phyllite, amphibolite (metabasite), talc schist, mica schist, calc schist intercalated with chert and red coloured, brecciated-like, occassionally fossiliferous (Ammonite-like forms, gastropoda, pelecypoda and macrofossil molds) marble, cherty marble in the upper sections (Figure 7). One of the distinguishing characteristics of the Söğütlüdere formation is that

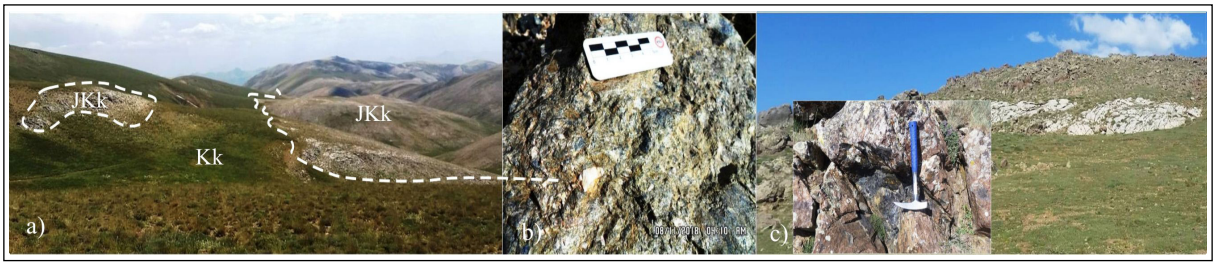

Figure 6- a) Unconformable contact between Kırkpınar formation (Kk) and Kırtepe formation (JKk), b) metaconglomerate within Kırkpınar formation, c) metaophiolite and marble blocks.

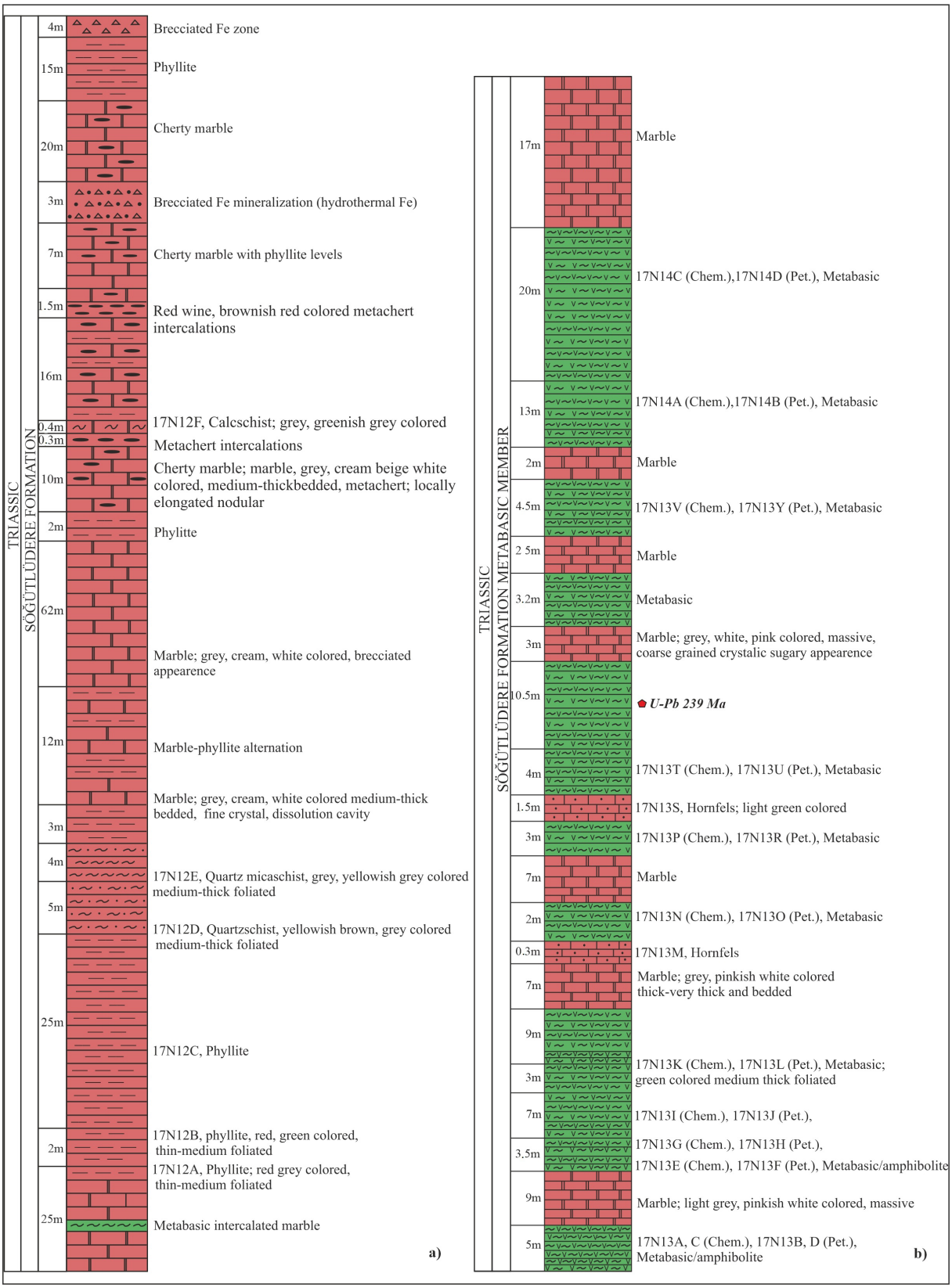

Figure 7- a) Measured section of Söğütlüdere formation (SW of the Özyurt Village; Adana-M33b1 sheet; UTM ED50 Zone 36 661558, 4200722), b) measured section of the metabasite member (East of Sazlıca, Söğütlüdere; Adana-M33a2 sheet; UTM ED50 Zone 36 4193697, 650638).

claret red-mottled coloured, thin to medium foliated, marble intercalated phyllites are most likely Early Triassic in age and predominantly forms the base of the unit. Cherty marble is gray, cream, beige in color, medium-thick bedded, fractured and contains chert in the form of nodules, staining and occasionally intercalations (Figure 8).

In the measured section of Söğütlüdere, which is the key site for the metabasite member, amphibolite/metabasites with light gray, pinkish white colored, thick-very thick bedded marble interlayers were observed (Figure 9). It was determined that the samples collected from the metabasite member are mostly composed of hornblende-plagioclase composition and weakly oriented amphibolites. These minerals are accompanied by clinopyroxenes in the hornfels-like, fine-grained granoblastic texture and non-oriented sections of metabasites, where they are more massive in texture and fine-grained.

Figure 8- a) General view from the Söğütlüdere formation, b) Mottled phyllites with marble intercalations derived from metamudstone-metasiltstone-metaclaystone, representing the Lower Triassic sections of the unit, c) Red colored, brecciated-like, occassionally fossiliferous (Ammonite-like forms, gastropoda, pelecypoda and macrofossil shell fragments) marble and d) cherty marbles.

Figure 9- General view from the metabasite member of the Söğütlüdere formation.

The metabasites in the unit consist of oriented, relatively coarse crystalline common amphibolites with fels appearance and fine grained massive texture. Diopsidefels detected in petrographic analysis shows nematogranoblastic texture and consists of clinopyroxene, plagioclase, epidote and small amounts of quartz and calcite minerals as main components. Clinopyroxene minerals are medium-grained, anhedral, commonly fissured, and they display green pleochroism. Plagioclase minerals are typical with polysynthetic twinning and are highly sericitized. Epidote minerals are typical with medium to fine grained, in anhedral forms with yellowish pleochroism. Small amounts of quartz and calcite minerals are medium grained and anhedral. Titanite minerals (sphene/leucoxene) are observed as accessory components in the rock. In addition, there are secondary calcite minerals as fillings in vein-shaped cracks in the rock. Amphibolite has nematogranoblastic texture and consists of medium-grained, prismatic, green pleochroic hornblendes and plagioclase feldspars with medium-grained, subhedral, occasionally sericitized, displaying polysynthetic twin lamellae. Quartz minerals are rarely observed and they are fine-grained and anhedral. Anhedral epidotes are medium-grained and rarely fine-grained. Titanites (sphene) are mostly common as accessory minerals in the rock and secondary calcite minerals are also present. The well-oriented rock was probably metamorphosed under the conditions of lower amphibolite facies. Clinoamphibole minerals in hornblende composition are medium-grained, subhedral, in prismatic forms and they display green pleochroism. Clinopyroxene minerals are medium-grained, anhedral, and heavily fissured. Plagioclase minerals are medium grained and highly sericitized. Quartzs are medium grained and anhedral. Calcite minerals are medium-grained and observed in anhedral forms. In addition, titanite minerals as accessory minerals are highly abundant and opaque minerals in the rocks are also highly observable. Calc-silicate fels have nematogranoblastic texture and consist of clinopyroxene, quartz and calcite minerals as the major components. Clinopyroxene minerals are medium-grained, anhedral, and heavily fissured. Quartz is medium grained and anhedral. Calcite minerals are medium and locally fine-grained, and they are in anhedral forms. Plagioclase minerals are common with their polysynthetic twinning. Clinozoisite minerals, which are rarely observed, are fine-grained and anhedral. Titanite minerals are found in the rock as an accessory component. The rock was probably metamorphosed under the lower amphibolite facies conditions. Tremolite actinolite schist has fibroblastic texture and consists of medium-grained, prismatic structure, light green pleochroism actinolite and colorless tremolite minerals as the major component. Plagioclase mineral has polysynthetic twin lamellae. The muscovite minerals, which are observed in small amounts, are fine-grained and flaky. Titanite minerals are observable in the rock as an accessory component. Minerals show parallel arrangement in the rocks with well-developed orientation. The rock was probably formed as a result of retrograde metamorphism of a basic rock under greenschist facies conditions. The Jurassic-Cretaceous Kırtepe formation with highly folded and fractured structure unconformably overlying the Kaleboynu formation and the Kızıldağ formation unconformably overlies the unit (Figure 10). The unit, which partially corresponds to a part of the Aşıgediği formation (Göncüoğlu, 1981) in the Niğde Massif, can be correlated with the Demirtepe formation (Beyazpirinç et al., 2020) in the Kırşehir Massif.

5. Geochemistry

Major, trace and rare earth element analyzes of a total of nine samples were carried out in Department of Mineral Analysis and Technology (MTA) to determine the geochemical and petrological properties of marble intercalated amphibolite/metabasites, which are distinguished at the member level within the Söğütlüdere formation. The graphs used in geochemical interpretations were generated using Excel and the GCDkit program, and the analysis results are given in Table 1.

5.1. Classification

In order to determine whether the amphibolite/metabasites separated at a member level in the Söğütlüdere formation, which might display sedimentary (para-amphibolite) or magmatic (ortho-amphibolite) origin, the results of the analyses were presented by the Ni-TiO_2 and Ni-Zr/TiO_2 graphs developed by Winchester et al. (1980) and Winchester

Figure 10- a) Unconformable contact relationship with the Jurassic-Cretaceous Kırtepe formation (JKk) overlying the Söğütlüdere formation (Trs) and quartzites derived from pure quartz arenite in the basement of quartzite along the contact, and b) Unconformable contact relationship with the late Permian Kızıldağ formation (Pk) located at the base of the Söğütlüdere formation.

and Max (1982). The results shown that the Ni contents of metabasites are between 91.00 and 377.60 ppm, the Zr contents are between 15.20 and 43.50 ppm, and the Zr/TiO_2 ratios vary between 0.0006 and 0.0016. As a result, the metabasites are originated from magmatic rocks following the plots into that can be seen in the trends which are created by the plots in the Ni-TiO_2 and Ni-Zr/TiO_2 graphs (Figure 11).

The samples of the Metabasite member samples of the Söğütlüdere formation (magmatic in origin) are classified by using the the total alkali versus silica (TAS) (Le Bas et al., 1986) diagram (Figure 12a), the origin rock of the metabasites is alkaline and basaltic in composition. In addition to this, the samples are classified as basalt and trachybasalt. Moreover, the loss on ignition (LOI) values of the analyzed samples vary between 0.85-5.05. Since it is possible to have some changes through major element oxide values of the rocks (especially SiO_2, CaO, K_2O and Na_2O) during hydrothermal alteration processes, metabasites are also classified in the Zr/Ti-Nb/Y diagram modified by Pearce (1996), in which elements that cannot be mobilized easily under low alteration and

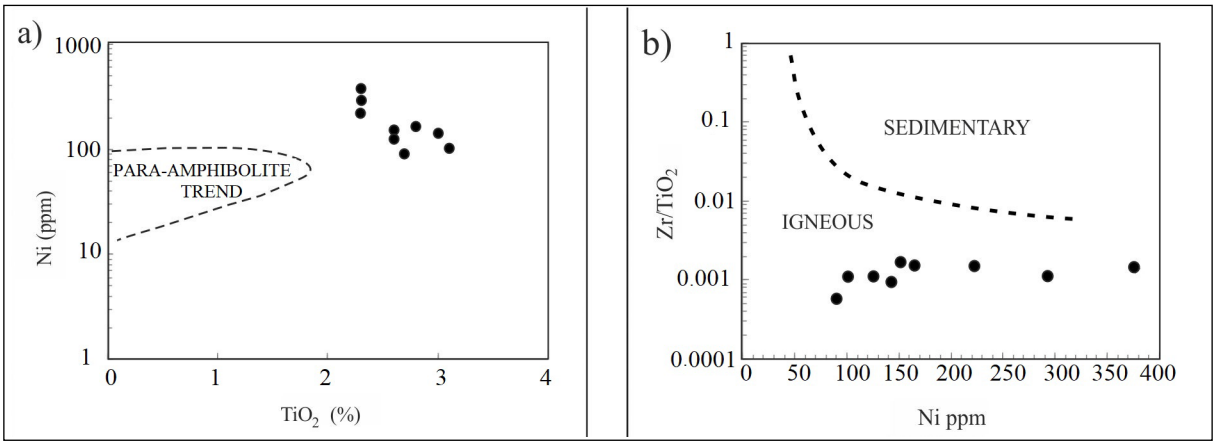

Figure 11- The rock samples of the Metabasite member of the Söğütlüdere formation; a) Winchester and Max (1982), b) Winchester et al. (1980) diagrams.

Table 1- Whole rock (major, trace and rare earth elements) chemical analysis results of the rock samples from the Metabasite member of the Söğütlüdere formation.

SAMPLE	17N13A	17N13C	17N13E	17N13G	17N13K	17N13N	17N13T	17N14A	17N14C
Major Oxides Wt. %									
SiO2	46.30	44.20	43.60	48.10	44.80	43.10	46.60	45.00	46.80
Al_2O_3	13.40	13.60	13.00	14.40	10.70	12.30	12.60	13.10	13.00
Fe_2O_3	11.30	13.30	11.90	11.50	12.10	11.00	12.90	12.30	13.00
CaO	12.40	12.60	14.00	9.40	13.90	15.40	12.00	13.50	11.50
MgO	3.90	5.70	5.40	5.30	8.30	4.90	7.00	5.90	6.30
Na2O	3.70	3.20	3.40	4.40	2.90	3.10	3.30	3.20	3.30
K2O	1.60	1.00	1.10	1.10	0.50	1.80	0.40	1.00	0.90
TiO2	2.30	3.10	2.60	2.70	2.30	2.30	3.00	2.80	2.60
MnO	0.10	0.20	0.20	0.10	0.20	0.10	0.20	0.20	0.20
P_2O_5	0.60	0.90	0.60	1.00	0.60	0.70	0.70	0.80	0.50
SrO	0.05	0.06	0.05	0.03	0.03	0.03	0.06	0.08	0.06
BaO	0.02	0.02	0.01	0.02	<0.01	0.03	0.01	0.03	0.03
Loss on ignition	4.20	2.05	4.00	1.80	3.30	5.05	0.85	1.90	1.55
Total	99.87	99.93	99.86	99.85	99.63	99.81	99.62	99.81	99.74
Trace Elements ppm									
Ba	160.00	164.60	118.00	133.90	60.80	162.90	76.80	211.00	165.10
Nb	35.90	58.40	60.40	70.70	45.50	41.30	60.30	62.10	40.80
Zr	25.40	34.70	43.50	15.20	31.80	34.90	28.80	42.70	28.70
Cs	1.10	0.30	0.40	0.20	0.20	0.30	<0.1	0.30	0.20
Ga	16.80	17.40	18.40	16.70	13.40	16.50	16.30	17.30	16.80
Hf	1.00	1.20	1.40	0.70	1.10	1.10	1.20	1.40	1.00
Rb	41.80	22.00	27.00	16.00	<10	24.00	<10	30.40	15.00
Sn	<10	<10	<10	<10	<10	<10	<10	<10	<10
Sr	463.00	428.50	415.00	247.30	249.60	256.90	470.80	665.00	485.40
Ta	1.90	3.00	2.70	3.50	2.20	1.90	2.90	2.60	2.10
Th	2.60	3.00	3.20	3.90	2.30	1.10	2.50	2.10	0.60
Tl	0.20	0.10	0.10	<0.1	<0.1	<0.1	<0.1	0.10	<0.1
U	<0.1	<0.1	<0.1	<0.1	<0.1	<0.1	<0.1	<0.1	<0.1
V	48.40	57.10	56.50	54.90	49.60	43.40	52.60	53.00	54.80
W	<10	<10	<10	<10	<10	<10	<10	<10	<10
Y	19.10	19.30	21.60	22.10	16.10	18.80	22.80	20.90	20.20
As	13.60	12.00	11.50	9.80	10.20	9.90	9.90	12.00	10.10
Be	1.80	1.50	2.20	1.50	2.10	1.60	2.30	1.30	2.30
Cd	0.10	0.10	<0.1	0.10	<0.1	0.10	0.10	<0.1	<0.1
Co	49.00	48.10	53.30	43.80	59.90	47.70	52.20	49.80	48.40
Cr	399.40	298	395.10	155	669	283	402	451.00	279
Cu	69.20	94.30	120.40	53.10	97.20	89.60	96.30	71.70	78.50
Ge	3.30	3.20	3.10	3.10	3.00	2.90	3.00	3.10	3.00
Mo	<0.1	<0.1	<0.1	<0.1	<0.1	<0.1	<0.1	<0.1	<0.1
Ni	293.10	100.80	151.50	91.00	377.60	222.80	143.20	164.90	125.60
Pb	<0.1	1.70	<0.1	<0.1	<0.1	<0.1	0.10	<0.1	<0.1
Sb	<0.1	<0.1	<0.1	<0.1	<0.1	<0.1	<0.1	<0.1	<0.1
Sc	29.10	32.80	35.90	24.10	31.20	23.00	35.00	32.40	40.00
Zn	127.50	129.10	125.80	129.80	123.70	132.10	132.80	136.60	121.00
La	16.90	27.00	27.60	31.10	19.70	19.50	27.80	28.80	17.80
Ce	38.90	56.40	57.20	64.40	42.70	40.40	60.40	57.30	37.70
Pr	4.10	5.60	5.70	6.60	4.40	4.30	6.30	5.70	4.20
Nd	17.30	22.30	22.30	25.90	17.00	17.80	24.40	22.10	16.30
Sm	3.80	4.30	4.50	5.00	3.60	3.70	4.90	4.40	3.50
Eu	1.40	1.40	1.70	1.60	1.20	1.40	1.60	1.60	1.40
Gd	4.70	4.50	5.10	5.20	3.80	3.90	5.70	4.50	4.30
Tb	0.70	0.60	0.70	0.70	0.50	0.60	0.80	0.60	0.60
Dy	3.60	3.40	4.10	4.20	3.00	3.30	4.30	3.40	3.70
Ho	0.60	0.60	0.70	0.90	0.60	0.60	0.80	0.60	0.70
Er	1.70	1.70	1.90	2.00	1.50	1.50	1.90	1.80	1.70
Tm	0.20	0.20	0.20	0.20	0.20	0.20	0.30	0.20	0.20
Yb	1.10	1.00	1.20	1.50	0.90	0.90	1.30	1.00	1.20
Lu	0.10	0.10	0.20	0.20	0.10	0.10	0.20	0.10	0.20

metamorphism conditions are used, indicating that the origin rock is determined as alkali basalt (Figure 12b).

5.2. Tectonic Environment

Tectonic discrimination diagrams are used in order to analyze the Metabasite member of the Söğütlüdere formation (Figure 13). The tectonic discrimination diagram proposed by Agrawal et al. (2008) (Figure 13a) that used trace elements (La, Sm, Yb, Nb and Th) which tend to not behave mobile in low grade alteration and metamorphism, and the tectonic discrimination diagram proposed by Cabanis and Lecolle (1989) diagram that used La/10-Y/15-Nb/8 ternary diagram (Figure 13b) for basic and ultrabasic rocks indicate that the Söğütlüdere formation is assosiated with the. Moreover, the Nb/Yb-TiO_2/Yb diagram (Pearce, 2008) was also used to determine tectonic environment that indicates the island arc basalts field with alkali composition are the tectonic environment (Figure 13c).

5.3. Distribution of Trace and Rare Earth Elements (REE)

The multi-element spider diagrams normalized to MORB and chondrite (Figure 14) were used to determine the magma source and nature of the Metabasite members of the Söğütlüdere formation. The main pattern shown that is formed by the samples in the MORB normalized multi-element spider diagram indicate the enrichment of large ion radius lithophile elements (Sr, K, Rb, Ba and Th) and the depletion of Zr, Hf, Y and Yb elements. Since crustal assimilation causes positive Zr and Hf anomalies during magma emplacement (Zhou et al., 2004), the negative Zr-Hf anomalies in the trace element diagram normalized according to MORB can be interpreted as the main magma might not have exposed to crustal contamination. The depletion of Y and Yb indicates the presence of amphibole and/or some garnet in the source (Figure 14a). It is also observed that the light rare earth elements (LREE) are enriched compared to heavy rare earth elements (HREE) in the multi-element distribution diagram normalized to chondrite (Figure 14b).

When the relations between the regional-geological location and the results of the chemical analyses chemical analysis results are examined, the rocks of the metabasite member of the Söğütlüdere formation can be interpreted as the first phase products of rifting that started with the breaking-away of the Tauride-Anatolide Platform in the Triassic period.

6. Geochronology

Two samples were used in order to determine the age of schist and amphibole of the Söğütlüdere formation, using the U/Pb zircon method. Zircons obtained from quartz-rich micaschist (17 N 16 sample) were used

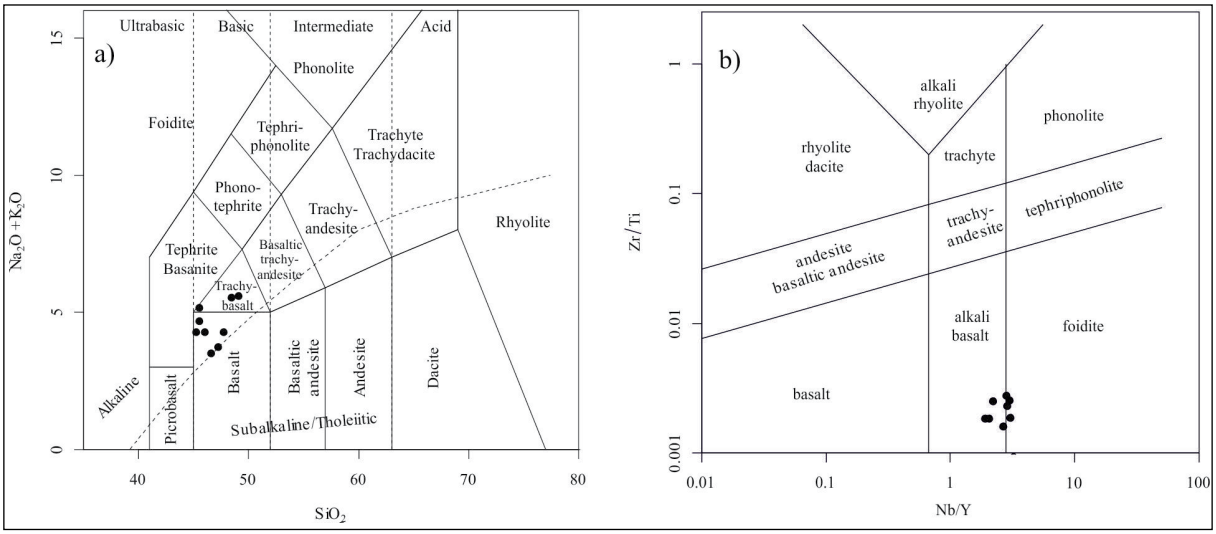

Figure 12- The rock samples of the metabasite member of the Söğütlüdere formation; a) Le Bas et al. (1986), b) Pearce (1996) classification diagrams.

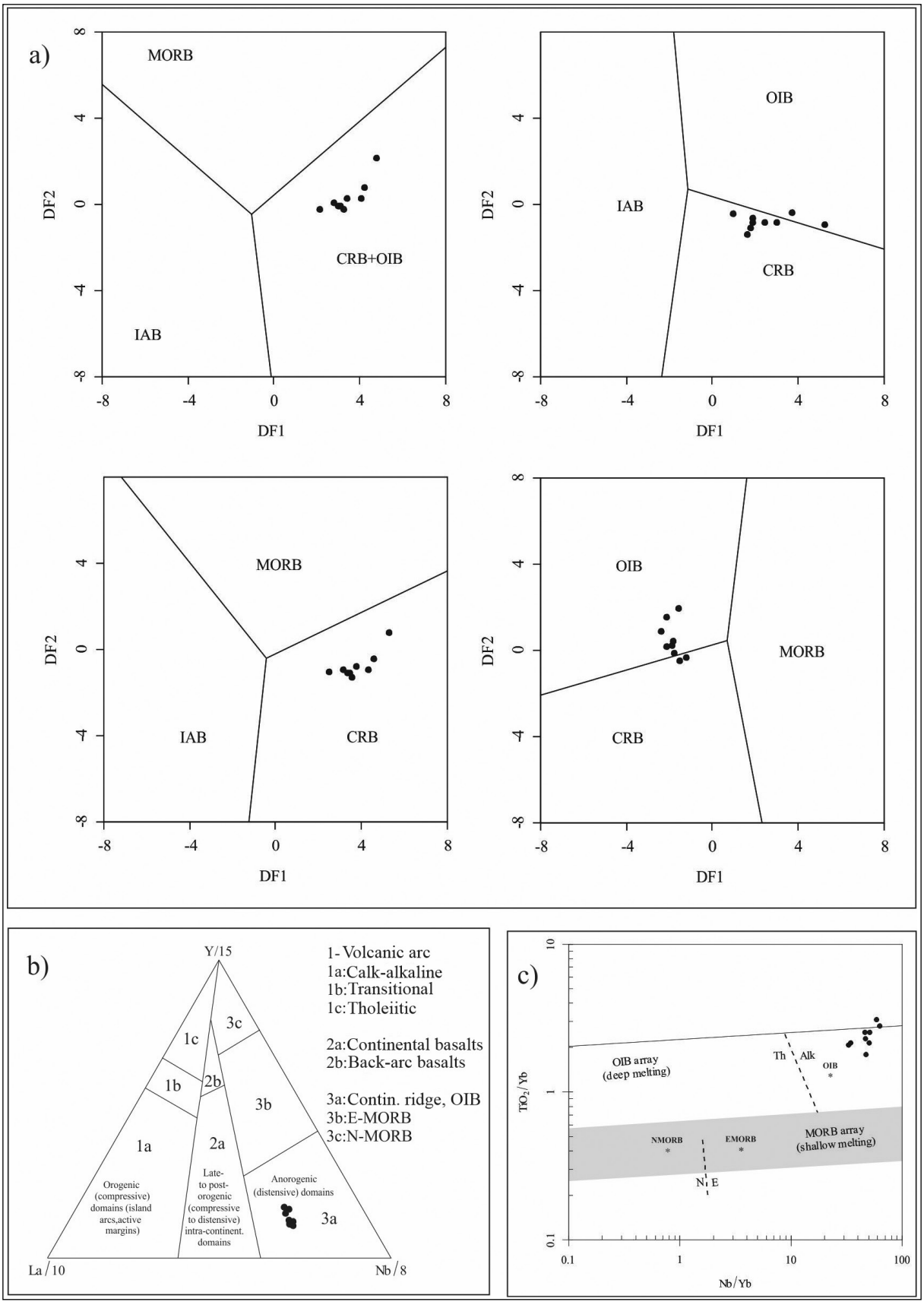

Figure 13- Rock samples of the Metabasite member of the Söğütlüdere formation in the tectonic environment discrimination diagrams; a) Agrawal et al. (2008), b) Cabanis and Lecolle (1989), c) Pearce (2008).

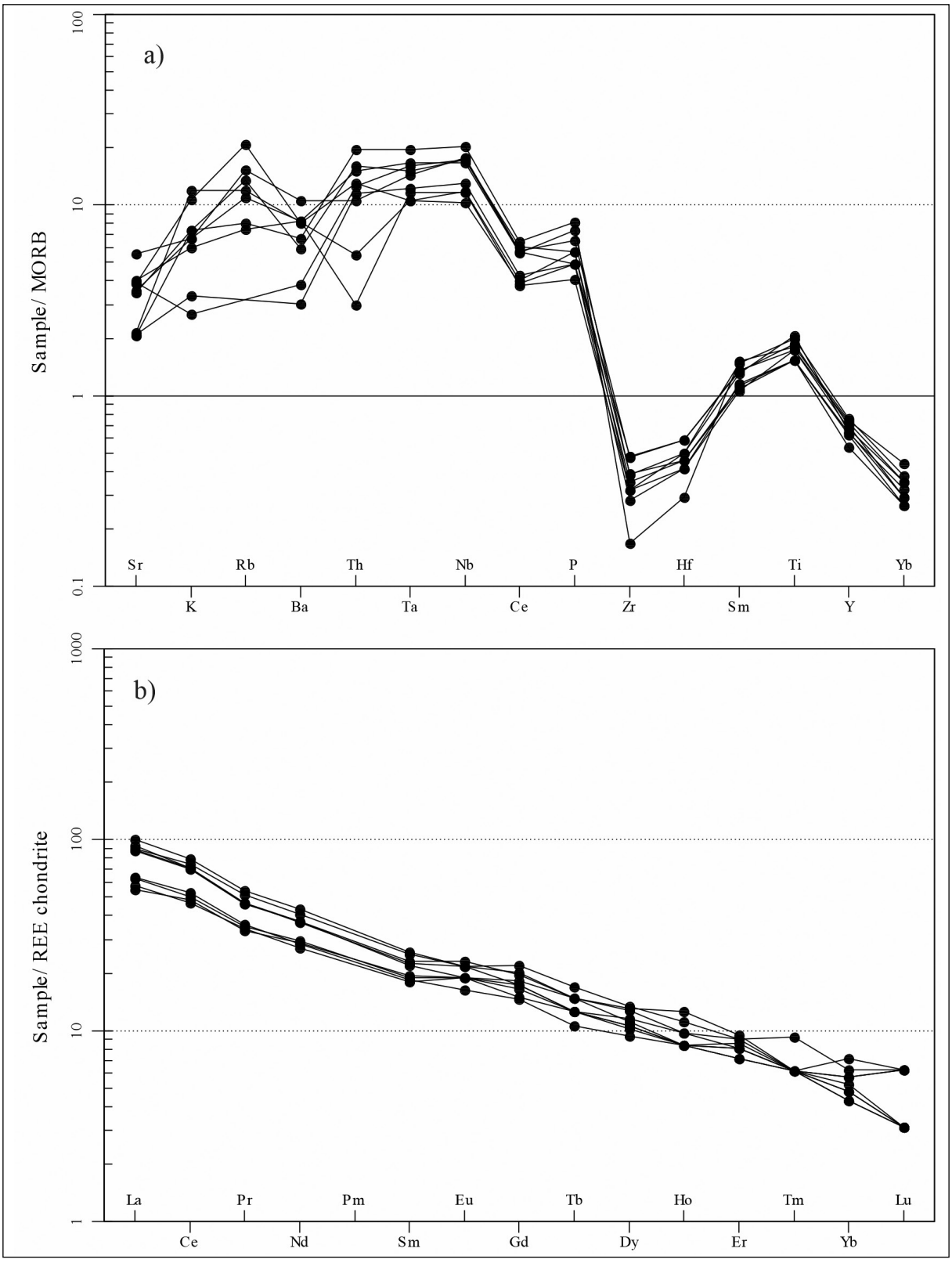

Figure 14- The rock samples of the Metabasite member of the Söğütlüdere formation; a) Multi-element spider diagram of trace elements normalized to MORB (Pearce, 1983), b) Multi-element spider diagram of rare earth elements normalized to chondrite (Boynton, 1984).

for the determine the U-Pb age with the help of LA-ICP-MS technique. The samples were collected from approximately 1 km north of Agapınar Hill and south of Gümüşler village (Adana M33 sheet; UTM ED50 Zone 36 0656960; 4199853). The sample is composed of biotite-muscovite-quartz-plagioclase-rutile-apatite-zircon and shows characteristic lepidoblastic texture. The zircons are acicular-like and not corroded much in the cathodoluminescence images of the examined sample (Figure 15). Grains with slightly rounded edges (gr 35) are also observed in the sample. Most of the grains have oscillating zoning reflecting the magmatic origin. Some grains (i.e gr 25 and 40) contain residual cores.

Analysis results of the samples are given in Table 2. From the analysis of 68 zircons selected from the sample, it was observed that 67 of them gave ages compatible between 90-110% ($^{206}Pb/^{238}U$ age/$^{207}Pb/^{235}U$ age *100) (Figure 16). Carboniferous zircons (301-342 Ma) (37%) (25 grains) and Neoproterozoic zircons (542-979 Ma) (28%) (19 grains) constitute the most abundant age group (Figure 17). Following those, 9% (6 grains) of Permian (253-292 Ma), 6% (4 grains) of Paleoproterozoic (1904-2100 Ma) and Ordovician of (453-473 Ma), 5% (3 grains) of Cambrian (512-532 Ma), 3% (2 grains) of Silurian (423-442 Ma) and Triassic (223-224 Ma) grains are present. Mesoproterozoic (1012 Ma) and Devonian (402 Ma) ages were obtained from only one zircon grain. Considering the two grains that yield the youngest age (223-224 Ma), the deposition age of the primary rock can be interpreted as Norian or earlier.

The amphibolite (metabasite) sample 17 N 18 was collected from 2 km SW of Keçikalesi Hill, located on the southern border of the study area (Adana M33 sheet; UTM ED50 Zone 36 0651685; 4193730). The rock is predominantly composed of hornblende. It also contains biotite, sphene apatite and opaque minerals. Nematoblastic texture resulting from the parallel orientation of the acicular-like amphiboles is observed in the sample. In order to find the crystallization age of the basaltic rock that forms the primary rock of amphibolite, zircon grains was tried to be enriched, but only two zircons were obtained from the sample. In the cathodoluminescence images of these two zircons (Figure 18), it is observed that the gr 2 zircon has acicular-like texture and oscillating zoning reflecting the magmatic origin. In the second grain (gr 1), only a small section reflecting magmatic zoning remains, while the other sections are zoneless and bright. This shows that this grain has been affected by metamorphism and its textural properties have disturbed. The age obtained based on these textural data was interpreted as the age of metamorphism.

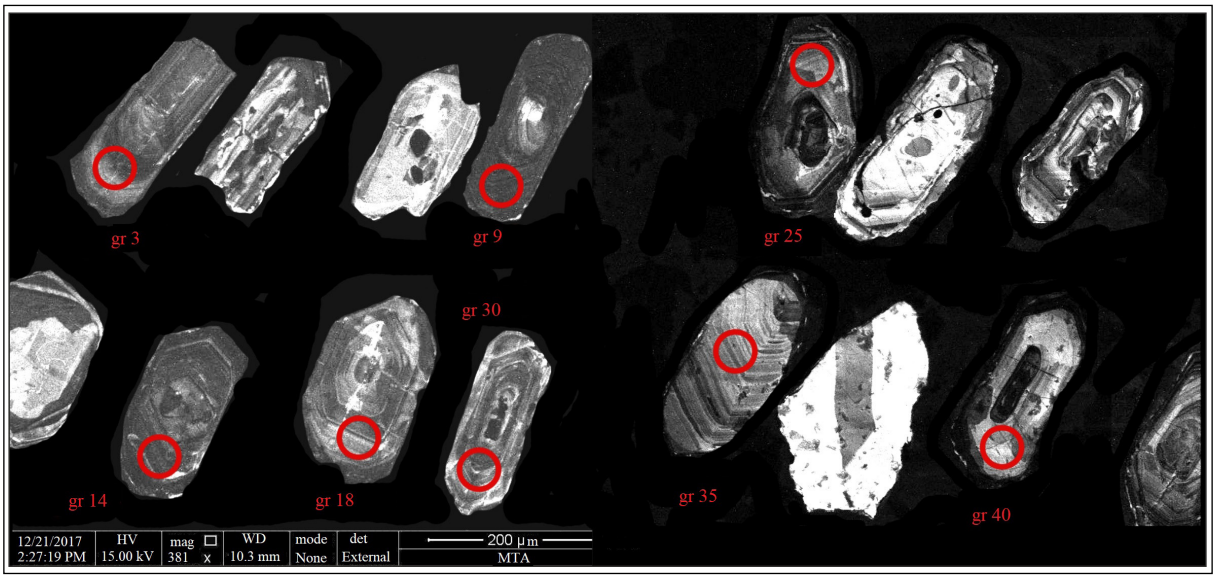

Figure 15- Cathodoluminescence photographs of zircons of quartzschist sample (17 N 16) and analysis spots in selected zircon grains for age determination.

Table 2- Isotope ratios of sample 17 N 16.

17 N 16 number isotope ratios									Ages (Ma)					
SAMPLE	206Pb•/ 207Pb•	± (%)	207Pb•/ 235U•	± (%)	206Pb•/ 238U	± (%)	Error correlation	206Pb•/ 238U	± (Ma)	207Pb•/ 235U•	± (Ma)	206Pb•/ 207Pb•	± (Ma)	% Concordia 6/8-7/5
gr 1	18.0312	1.2796	0.2684	1.7869	0.0351	1.2473	0.6980	222.5	2.7	241.5	3.8	429 .8	28.5	92
gr 2	18.3990	0.7063	0.2654	1.2802	0.0354	1.0678	0.8341	224.4	2.4	239.0	2.7	384.6	15.9	94
gr 3	18.8394	0.7398	0.2931	1.3880	0.0401	1.1744	0.8461	253.2	2.9	261.0	3.2	331.2	16.8	97
gr 4	14.2255	2.2493	0.4007	2.6097	0.0414	1.3235	0.5071	261.3	3.4	342.2	7.6	936.1	46 .1	76
gr 5	18.0575	1.2200	0.3445	1.5557	0.0451	0.9653	0.6205	284.6	2.7	300.6	4.0	426 .6	27.2	95
gr 6	17.8689	1.1290	0.3569	1.7548	0.0463	1.3435	0.7656	291.6	3.8	309.9	4.7	449 .9	25.1	94
gr 7	18.7095	0.6860	0.3518	1.1575	0.0478	0.9323	0.8055	300.7	2.7	306.1	3.1	346.9	15.5	98
gr 8	18.5659	0.9941	0.3562	1.5904	0.0480	1.2415	0.7806	302.1	3.7	309.4	4.2	364.3	22.4	98
gr 9	18.7384	0.7106	0.3588	1.2253	0.0488	0.9982	0.8147	307.0	3.0	311.3	3.3	343.4	16.1	99
gr 10	18.6591	0.5217	0.3641	1.0264	0.0493	0.8839	0.8612	310.2	2.7	315.3	2.8	353.0	11.8	98
gr 11	18.6286	0.6831	0.3663	1.2864	0.0495	1.0900	0.8473	311.5	3.3	316.9	3.5	356.7	15.4	98
gr 12	18.7706	0.7390	0.3643	1.3765	0.0496	1.1613	0.8437	312.2	3.5	315.4	3.7	339.5	16.7	99
gr 13	18.7375	0.6931	0.3676	1.225 1	0.0500	1.0101	0.8246	314.3	3.1	317.8	3.3	343.5	15.7	99
gr 14	19.0143	0.7577	0.3698	1.3580	0.0510	1.1270	0.8299	320.8	3.5	319.5	3.7	310.3	17.2	100
gr 15	19.0768	0.9015	0.3687	1.5717	0.0510	1.2874	0.8191	320.9	4.0	318.7	4.3	302.8	20.5	101
gr 16	18.9931	1.1023	0.3730	1.3177	0.0514	0.7220	0.5479	323.1	2.3	321.9	3.6	312.8	25.1	100
gr 17	18.9882	0.7490	0.3735	1.4990	0.0515	1.2985	0.8662	323.5	4.1	322.2	4.1	313.4	17.0	100
gr 18	19.0954	0.6534	0.3726	1.3736	0.0516	1.2083	0.8796	324.5	3.8	321.6	3.8	300.6	14.9	101
gr 19	18.8406	0.8230	0.3789	1.3972	0.0518	1.1290	0.8081	326.0	3.6	326.2	3.9	331.1	18.7	100
gr 20	18.6996	0.7232	0.3823	1.2943	0.0519	1.0734	0.8293	325.5	3.4	328.7	3.6	348.1	16.3	99
gr 21	18.5120	0.8065	0.3868	1.5797	0.0519	1.3583	0.8599	326.5	4.3	332.0	4.5	370.8	18.1	98
gr 22	18.7850	0.8483	0.3816	1.2948	0.0520	0.9782	0.7555	326.9	3.1	328.2	3.6	337.8	19.2	100
gr 23	18.2897	0.8611	0.3944	1.4118	0.0523	1.1188	0.7925	328.8	3.6	337.5	4.1	398.0	19.3	97
gr 24	18.3783	1.4207	0.5327	1.6956	0.0710	0.9256	0.5459	442 .4	4.0	433 .6	6.0	387.1	31.9	102
gr 25	17.2123	0.6596	0.6102	1.2637	0.0762	1.0779	0.8530	473 .4	4.9	483 .7	4.9	532.5	14.4	98
gr 26	17.3014	1.9686	0.6588	2.3061	0.0827	1.2012	0.5209	512.2	5.9	513.9	9.3	521.2	43.2	100
gr 27	16.5881	1.4880	0.7034	1.7386	0.0847	0.8992	0.5172	523.9	4.5	540.8	7.3	612.8	32.1	97
gr 28	17.0671	1.0978	0.6940	1.5104	0.0859	1.0374	0.6868	531.5	5.3	535.2	6.3	551.0	24.0	99
gr 29	17.5189	0.8791	0.6893	1.3120	0.0876	0.9739	0.7423	541.5	5.1	532.4	5.4	493 .7	19.4	102
gr 30	16.6802	0.4470	0.7683	0.9069	0.0930	0.7892	0.8701	573.2	4.3	578.8	4.0	600.9	9.7	99
gr 31	15.9337	0.8860	0.8126	1.6329	0.0940	1.3717	0.8400	578.9	7.6	603.9	7.4	699.2	18.9	96
gr 32	16.4480	0.7987	0.8472	1.4905	0.1011	1.2584	0.8443	620.9	7.4	623.1	6.9	631.2	17.2	100
gr 33	15.7785	1.0693	1.0599	1.3738	0.1213	0.8625	0.6278	738.3	6.0	733.8	7.2	720.0	22.7	101
gr 34	8.143 1	0.6641	5.6289	1.3298	0.3326	1.1521	0.8664	1850.9	18.5	1920.5	11.5	1996.6	11.8	96
gr 35	18.8049	1.3748	0.3032	2.3747	0.0414	1.9362	0.8154	261.3	5.0	268.9	5.6	335.4	31.1	97
gr 36	18.5560	0.4013	0.3076	1.1608	0.0414	1.0892	0.9383	261.6	2.8	272.3	2.8	365.5	9.0	96
gr 37	18.6095	0.6384	0.3235	1.1626	0.0437	0.9717	0.8358	275 .6	2.6	284.6	2.9	359.0	14.4	97
gr 38	18.7040	0.5981	0.3649	1.2222	0.0495	1.0659	0.8721	311.6	3.2	315.9	3.3	347.6	13.5	99
gr 39	18.5132	0.7191	0.3729	1.1979	0.0501	0.9580	0.7998	315.1	2.9	321.8	3.3	370.7	16.2	98
gr 40	19.0286	0.6519	0.3648	1.2612	0.0504	1.0796	0.8561	316.8	3.3	315.8	3.4	308.6	14.8	100
gr 41	18.7707	0.5561	0.3702	1.0185	0.0504	0.8532	0.8378	317.1	2.6	319.8	2.8	339.5	12.6	99
gr 42	18.9276	0.6718	0.3674	1.3087	0.0505	1.1231	0.8582	317.3	3.5	317.7	3.6	320.7	15.3	100
gr 43	18.9005	0.6472	0.3764	1.0706	0.0516	0.8528	0.7966	324.5	2.7	324.4	3.0	323.9	14.7	100
gr 44	18.7608	0.7296	0.3826	1.2919	0.0521	1.0662	0.8253	327.3	3.4	328.9	3.6	340.7	16.5	99
gr 45	19.0557	0.7013	0.3931	1.1803	0.0543	0.9493	0.8043	341.2	3.2	336.6	3.4	305.3	16.0	101
gr 46	16.8281	0.7336	0.5272	1.2282	0.0644	0.9851	0.8020	402 .2	3.8	430.0	4.3	581.8	15.9	94
gr 47	16.8797	0.9412	0.5543	1.3166	0.0679	0.9207	0.6993	423 .4	3.8	447 .8	4.8	575.1	20.5	95
gr 48	17.3661	0.9232	0.5771	1.3556	0.0727	0.9926	0.7322	452 .5	4.3	462 .6	5.0	513.0	20.3	98
gr 49	17.5598	0.6366	0.5753	1.3201	0.0733	1.1564	0.8760	456 .0	5.1	461.4	4.9	488.6	14.1	99
gr 50	17.5902	0.7147	0.5930	1.1788	0.0757	0.9374	0.7952	470.3	4.3	472 .8	4.5	484 .8	15.8	99
gr 51	17.1681	0.6047	0.7050	1.1999	0.0878	1.0364	0.8637	542.6	5.4	541.8	5.0	538.1	13.2	100
gr 52	17.5675	1.2434	0.7126	1.8607	0.0908	1.3842	0.7439	560.4	7.4	546.3	7.9	487 .6	27.4	103
gr 53	16.8581	0.6371	0.7523	1.1544	0.0920	0.9627	0.8339	567.5	5.2	569.6	5.0	577.8	13.8	100
gr 54	17.3496	0.9455	0.7312	1.3545	0.0920	0.9699	0.7161	567.6	5.3	557.3	5.8	515.1	20.8	102
gr 55	16.8241	0.7006	0.7587	1.2697	0.0926	1.0588	0.8340	571.0	5.8	573.2	5.6	582.2	15.2	100
gr 56	16.5935	0.6732	0.7853	1.2257	0.0945	1.0243	0.8357	582.4	5.7	588.5	5.5	612.1	14.5	99
gr 57	16.8288	0.7002	0.7990	1.1253	0.0976	0.8810	0.7828	600.1	5.0	596.3	5.1	581.6	15.2	101
gr 58	17.4206	2.2674	0.8180	2.6551	0.1034	1.3815	0.5203	634.3	8.3	606.9	12.1	506.1	49.9	105
gr 59	15.8591	0.7981	1.0076	1.1225	0.1159	0.7894	0.7032	707.2	5.3	707.7	5.7	709.2	17.0	100
gr 60	15.7177	0.6148	1.0294	1.0855	0.1174	0.8946	0.8241	715.6	6.1	718.6	5.6	728.2	13.0	100
gr 61	14.9947	0.8572	1.1786	1.2408	0.1282	0.8971	0.7230	777.8	6.6	790.7	6.8	827.2	17.9	98
gr 62	13.9566	0.8013	1.6199	1.3584	0.1640	1.0969	0.8075	979.2	10.0	978.0	8.5	975.1	16.3	100
gr 63	13.9518	0.7371	1.4430	1.6049	0.146 1	1.4256	0.8883	878.9	11.7	907.0	9.6	975.9	15.0	97
gr 64	13.8720	0.7699	1.6899	1.1580	0.1701	0.8650	0.7470	1012.6	8.1	1004.7	7.4	987.5	15.7	101
gr 65	13.8123	0.6730	1.6290	0.9840	0.1633	0.7179	0.7295	974.8	6.5	981.5	6.2	996.3	13.7	99
gr 66	8.5774	0.6563	5.3987	1.0497	0.3360	0.8192	0.7804	1867.4	13.3	1884.7	9.0	1903.7	11.8	99
gr 67	8.3839	0.7987	5.2208	1.4162	0.3176	1.1695	0.8258	1778.0	18.2	1856.0	12.1	1944.6	14.3	96
gr 68	7.6819	0.6584	6.7624	1.1874	0.3769	0.9882	0.8322	2061.9	17.4	2080.8	10.5	2099 .6	11.6	99

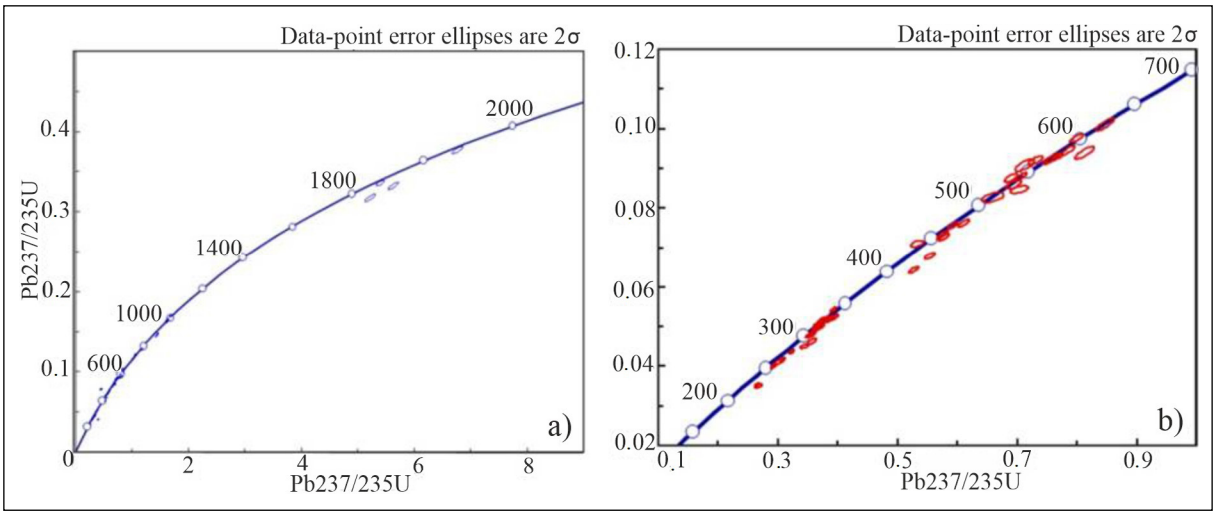

Figure 16- a) All zircons of the sample 17 N 16 on the concordia diagram, and b) the grains younger than 600 Ma on the concordia diagram.

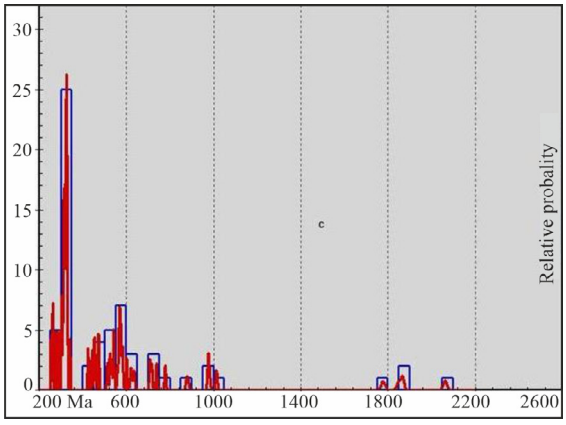

Figure 17- Histogram of sample 17 N 16 showing the age distribution.

An age of 238.5±2.8 Ma (Middle Triassic) was obtained from a zircon grain (gr 2) with a magmatic texture with 99% compatibility (Table 3; Figure 19). The other zircon grain (gr 1) yields an age of 82.7±0.8 Ma (Campanian). It is observed that the first age is compatible with the Triassic depositional age obtained from the previous sample. Campanian can interpreted as metamorphic age considering the tectono-metamorphic evolution of the region.

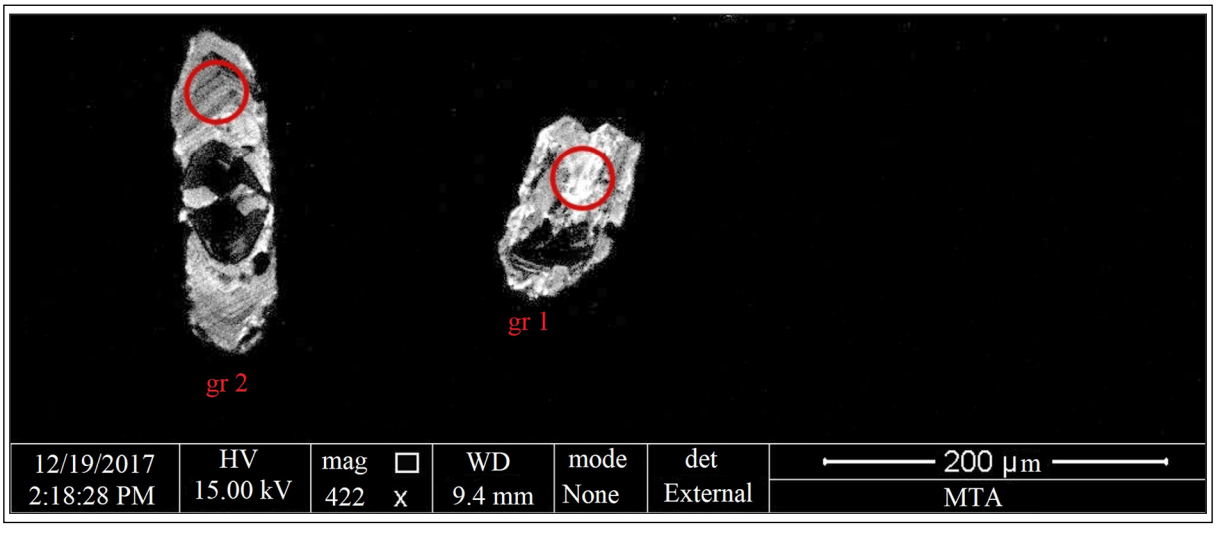

Figure 18- The cathodoluminescence photographs of the zircons of the 17 N 18 amphibolite sample and the analysis spots through the age determination.

Table 3- Isotope ratios of sample 17 N 18.

Isotope Ratios							Apparent Ages (Ma)							
206Pb*	±	207Pb*	±	206Pb*	±	error	206Pb*	±	207Pb*	±	206Pb*	:!:	Best age	±
207Pb*	(%)	235U*	(%)	238U	(%)	corr_	238U*	(Ma)	235U	(Ma)	207Pb*	(Ma)	(Ma)	(Ma)
19.0356	6.0	0.0935	6.1	0.0129	1.0	0.16	82.7	0.8	90.8	5.3	307.7	137.5	82.7	0.8
19.4177	0.7	0.2676	1.3	0.0377	1.2	0.87	238.5	2.8	240.7	2.9	262.3	15.0	238.5	2.8

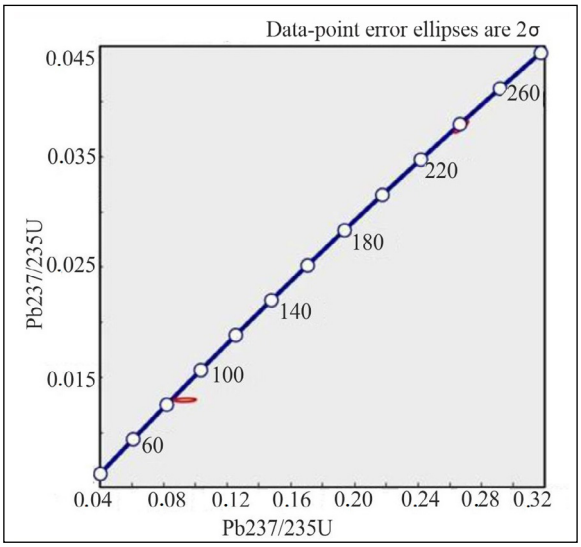

Figure 19- Two zircons aged in sample 17 N 18 on the concordia diagram.

7. Results

The findings obtained from this study and their meaning in terms of regional tectonics can be grouped under four headings:

7.1. Stratigraphy of the Niğde Massif

Paleozoic-Mesozoic was given for the age of the metamorphics of the Niğde Massif which displays very wide range, and it was accepted that it consists of three formations with a conformable contact relationship with each other in previous studies. In this study, the Late Devonian, Carboniferous-early Permian and late Permian deposits representing a conformable and transitional succession and a total of six Triassic, Jurassic-Cretaceous and Late Cretaceous formations overlying and unconformably separated from each other were distinguished. Niğde group by Göncüoğlu (1981) and the Kaleboynu and Gümüşler formations defined by Atabey et al. (1990) under Niğde metamorphic sequence were generally distinguished in the same way in this study, although there are minor differences in the definition. However, a significant part of the marbles, which is included in the Gümüşler formation by Atabey et al. (1990), was distinguished as the Jura-Cretaceous Kırtepe formation, which unconformably overlies the older units in the metamorphic succession. On the other hand, previous researchers have defined the Aşıgediği formation considering very different lithofacies together; however, four formations within this unit have been defined in this study as the Triassic Söğütlüdere, Jurassic-Cretaceous Kırtepe, Late Cretaceous Kırkpınar formation and late Permian Kızıldağı formation seperated with unconformable contacts (Figure 20). Thus, the stratigraphy of the Niğde Massif is completely renewed and the Late Devonian-Late Cretaceous formation partly separated from each other by unconformities that have been distinguished.

7.2. Age and Tectonic Environment of Basic Volcanism

The unit (Söğütlüdere formation) of the amphibolite sample used for radiometric dating. This unit is unconformably underlain by the marbles of late Permian Bozçaldağ formation and is unconformably overlain by the Jurassic-Cretaceous marbles. Furthermore, it displays characteristics that can be correlated with similar Lower-Middle Triassic successions in the Taurus Mountains (Geyikdağı unit, Aladağ nappe, also Bodrum nappe, Bolkardağı nappe). The 239 Ma (Middle Triassic) zircon U/Pb age obtained from the amphibolite sample is consistent with these stratigraphic data and shows that the common basic magmatism in the Niğde Massif is Triassic in broad sense. The geochemical results of the amphibolites indicate that the basic magmatism is associated with alkaline composition and displays anorogenic character. Geochemical, geochronological

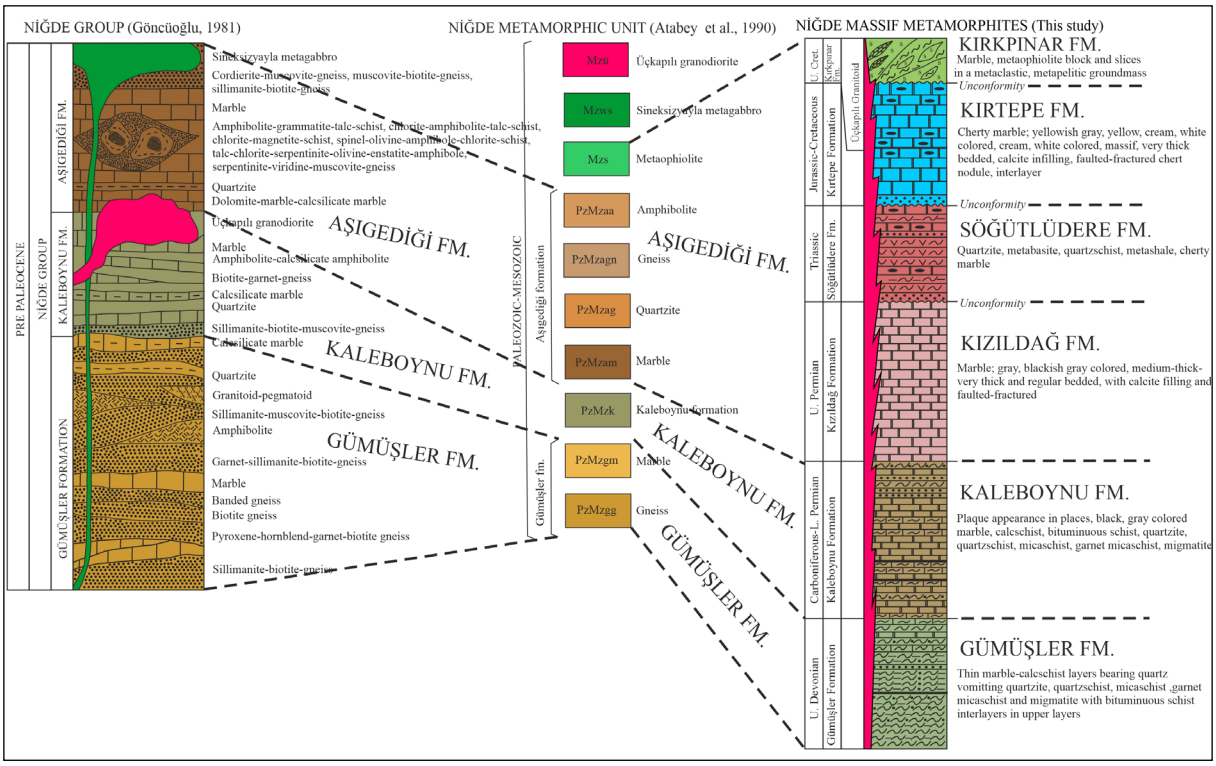

Figure 20- Correlation sections of the Niğde Massif metamorphics.

data and stratigraphic observations show that volcanism during the Triassic indicates an extensional tectonic environment that developed in a continental crust.

7.3. Source Rock Problem of the Triassic Metaclastics

In recent years, studies on the determination of source rocks of clastic rocks have become very popular and many articles have been published on this subject. Detritic zircon geochronology has been widely used for these type of further provenance studies (Fedo et al., 2003), which helps to approach paleogeographic position of a tectonic unit in a given period of time. The Istanbul Zone (Okay et al., 2011), Sakarya Zone (Akdoğan et al., 2019; Ustaömer et al., 2016), Taurus (Ustaömer et al., 2019), Menderes (Zlatkin et al., 2013) and Bitlis (Ustaömer et al., 2012) massifs and Karaburun-Chios (Meinhold et al., 2008; Löwen et al., 2017) have been especially studied using this technique. For this purpose, clastic zircon dating was carried out using the U/Pb method from a schist sample of the Middle-Late Triassic Söğütlüdere formation in the Niğde Massif. Results of 67 analysis spots with 90-110% concordance are as they are given; 4 grains of (6%) Paleoproterozoic (1904-2100 Ma), 1 grain of Mesoproterozoic (1012 Ma), 19 grains of (29%) Neoproterozoic (542-979 Ma), 3 grains of (5%) Cambrian (512-532 Ma), 4 grains of (6%) Ordovician (453-473 Ma), 2 grains of (3%) Silurian (423-442 Ma), 1 grains of Devonian (1%) (402 Ma), 25 grains of (38%) Carboniferous (301- 342 Ma), 6 grains of (9%) Permian (253-292 Ma) and 2 grains of (3%) Triassic (223-224 Ma) (Figure 17). Neoproterozoic (29%) and Carboniferous (38%) zircons constitute the two dominant populations in the rock. Some zircons of the Paleozoic period are also present apart from those. Among the Precambrian zircons in the sample, Neoproterozoic ones constitute the dominant group, while 4 Paleoproterozoic zircons accompany them. The sample clearly contains voids in terms of Mesoproterozoic zircon (1 unit) (Figure 17). It is commonly accepted that the Gondwana completed its amalgamatiom process in the early Cambrian (Torsvik and Cock, 2013). Magmatic and metamorphic processes along the northern margin of supercontinent has critical importance to understand the positions of primary paleogeographic positions of the microplates, which was broken away from that margin and drifted

towards northerly. The region around the Amazon Craton to the west is characterized by the widespread presence of Mesoproterozoic (1600-1000 Ma) zircons associated with the Greenville Orogeny (1250-980 Ma). The West African Craton is defined by the presence of approximately 2000 Ma of magmatic activity (Altumi et al., 2013). The Arabian-Nubian Shield and the Saharan Metacraton are characterized by the presence of extensive Neoproterozoic (Cryogenic-Ediacaran) magmatism (Johnson and Kattan, 2007; Johnson et al., 2011; Robinson et al., 2014; references therein) towards east especially throughout the Northeast Africa. Considering the zircon population in the sample used for geochronological studies, 2000 Ma and 1250-980 Ma (Mesoproterozoic) grains are extremely poor in terms of zircon (2 in total), on the contrary, Neoproterozoic zircons constitute the second dominant peak with a rate of 29%. These data point to the Saharan Metacraton and the Arabian-Nubian Shield in Northeast Africa as the source rock of the Precambrian zircons for the sample of the Söğütlüdere formation. This possibility is also compatible with the modern idea of the north of Arabia, which was proposed for the pre-Triassic paleogeographic location of the Taurus Mountains based on various geological data (Şengör and Yılmaz, 1981; Şengör et al., 1984; Stern, 1994; Stampli and Borel, 2002; Monod et al., 2003; Gessner et al., 2004; Linnemann et al., 2007; Ustaömer et al., 2009). The most dominant zircon assemblage in the sample is Carboniferous with a rate of 38%.

As well documented (Okay and Topuz, 2017, references therein), the southern margin of Laurussia is characterized by the Pelagonian Zone in Greece (315-275 Ma; Anders et al., 2007) and the Cyclades (317 Ma; Engel and Reischmann, 1998) (Central European crystalline basements in the West), Caucasus in the east (331-325 Ma; Gamkrelidze et al., 2011), the Carboniferous high temperature metamorphism of the Variscan basement of the Sakarya Zone (345-310 Ma; Topuz et al., 2007; Ustaömer et al., 2013) and existence of accompanying widespread syn-post metamorphic plutons (325-310 Ma; Topuz et al., 2010, 2020; Ustaömer et al., 2013). In recent years, Carboniferous zircons form an extremely dominant assemblage, especially in the zircon dating of the Taurus (Ustaömer et al., 2019), Konya mélange (Löwen et al., 2018, 2019) and Karaburun-Chios mélange (Löwen et al., 2017) clastics and the Variscan crystalline basement was predicted as the source rock and the southern edge of Laurussia as the paleogeographic location based on the data obtained. However, new findings obtained in recent years indicate the presence of Carboniferous magmatism, which is generally associated with a short-term subduction or extensional regime in the northern margin of the Gondwana (Teke Dere; Robertson and Ustaömer, 2009; Feke unit/Saimbeyli; Dalkılıç, 2009; Çataloturan/Eastern Taurus; Göncüoğlu et al., 2007; Afyon Zone; Candan et al., 2016; Binboğa metamorphics; Robertson et al., 2021). Ustaömer et al. (2019) revealed that these zircons do not match with the Laurussian magmatic activity based on the Hf isotope values of the zircons selected in Triassic sandstones of the Taurus Mountains. When the stratigraphic similarities of the Niğde Massif metamorphites with the Taurus units and the data that the Anatolide-Tauride Block remained connected to Gondwana until the Triassic are evaluated together, Carboniferous magmatism development on the northern margin of the Gondwana can be predicted as the source rock of the zircons in the Söğütlüdere formation clastics. In the aged sample, the presence of Ordovician, Silurian and Devonian zircons was also detected in addition to these zircons. Until recently, problems have been experienced in the source rock interpretations of these aged detrital zircons in the Taurus units. However, radiometric data in recent years have revealed the presence of magmatism at these ages on the northern margin of the Gondwana. Topuz et al. (2021) suggested the 430-440 Ma (Late Ordovician-Silurian) aged anorogenic metagranites associated with the opening process of the Paleotethys Ocean in Ağrı/Taşlıçay. The presence of the Ordovician metagranites (467 Ma) is also known in the Tavşanlı Zone (Okay et al., 2008). In addition to these, two Triassic zircon grains were dated in the sample. Widespread presence of Triassic magmatic activity in the north of Gondwana (Karaburun 247 Ma, Akal et al., 2011; Menderes Massif 246-235 My, Koralay et al., 2001; Afyon Zone 250-229 Ma, Akal et al., 2012; Özdamar et al., 2013).) has been documented in many studies.

The Northeast African/Saharan Metacraton and the Arabian-Nubian Shield can be interpreted as the source area of the Precambrian zircons from the sample dated based on the data and results presented above.

For the Paleozoic-Triassic zircons in the sample, the periodic extensional regimes and magmatic activities associated with short-term subduction on the northern margin of Gondwana can be suggested as the source rocks.

7.4. The Position of Basic Volcanism in Regional Tectonics

The similarities of the Paleozoic succession of the Niğde Massif within the Kırşehir Block, which was defined as the continental block in previous studies, to the Arabian Plate (Perinçek, 1990) and Taurus units (Özgül, 1976; Özgül and Kozlu, 2002) indicate that this continental block remained attached to north of the Gondwana during the Paleozoic. The findings until nowadays show that the northern margin of the Gondwana has been affected by periodic extensional regime since the Early Paleozoic and short-term subduction in the Carboniferous (Candan et al., 2016; Robertson et al., 2021). As a result of these extension processes, it is widely accepted that continental fragments broke away from the north of the Gondwana during the Early Paleozoic-Early Mesozoic interval and were drifted northward and amalgamated to the continental fragments in the north (the fragments constituing the Laurussia in broad sense) (Von Raumer and Stampfli, 2008; Stampfli et al., 2013; Torsvik and Cocks, 2013 and references therein). It is suggested that Avalonia was the first continental fragment broken away from the north of the Gondwana (the part of Amazonia and West African cratons) associated with the opening of the Reich Ocean in the Middle Ordovician (~470 Ma), which is resulted in Caledonian Orogeny, and amalgamated with Laurentia and Baltica to form Laurussia in the north during late Silurian (~420 Ma) (Stampfli and Borel, 2002; references in Von Raumer and Stampfli, 2008). The second continental fragment broke away from the northern part of Gondwana is called the Armorica Continent, especially in Central Europe, although it is defined by different names in many studies (Stampfli and Borel, 2002; Stampfli et al., 2013 and references therein). It is generally accepted this continental fragment was broken away from the North Africa and breaking-away processes resulted in the opening of the Paleotethys Ocean. However, the timing of the opening of the Paleotethys Ocean and whether this opening occurred at the same time along the North Africa is still controversial today. New geochemical and geochronological findings indicate that this opening took place in the Balkans and Türkiye around 440 Ma (Late Ordovician-early Silurian) (Topuz et al., 2020, 2021). This continental fragment collided with Laurussia in the north and Pangea was formed during the Late Carboniferous in the following stage (Muttoni et al., 2003; Stampfli et al., 2013). High-grade metamorphism and accompanying widespread magmatism (Variscan Orogeny) commonly observed in Central Europe and its eastern extension, Balkan countries, Sakarya Zone and Caucasus (Okay and Topuz, 2017) are associated with this collision and supercontinent formation. The extension process that was present along the northern margin of the Gondwana in the Early Triassic is associated with the opening of the Neotethys oceans, which largely shaped the present geological structure of the Eastern Mediterranean, and the breaking-away of the Anatolide-Tauride Block from the Gondwana. It is suggested that the Neotethys Ocean system was formed by the formation of two new oceans as the northern and southern branches in the previous studies (Şengör and Yılmaz, 1981; Okay et al., 2006). However, the new findings especially from the Sakarya Zone in recent years indicate Paleotethys Ocean subducted beneath southern margin of the Laurassia during the late Carboniferous or late Permian (Topuz et al., 2004) towards north and commenced to closure and it is suggested that this oceanic area existed until the continental collision in the Eocene (Okay, 2000; Okay and Nikishin, 2015; Okay et al., 2020). In summary, the current dominant suggestion is that the northern branch of the Neotethys Ocean did not open and the Anatolide-Tauride Block was broken away from the Gondwana as a result of the Southern Branch of the Neotethys Ocean opening in the Triassic (Göncüoğlu et al., 2003; Okay et al., 2006). The Kırşehir Block is interpreted as an isolated continental fragment within the Tethys Ocean in almost all of the paleogeographic maps within this general tectonic framework (Barrier et al., 2018). The boundary between the Kırşehir Block and the Anatolide-Tauride Block is defined as a suture zone in the tectonic map of Türkiye (Okay and Tüysüz, 1999). This boundary corresponds a former subduction zone considering the suggestions of the Late Cretaceous high-pressure metamorphism belt (Afyon Zone) along this boundary (Candan et al.,

2005; Pourteau et al., 2010) and the ophiolitic rocks in Mersin region derived from the same area (Parlak ve Robertson, 2004) and it indicates existence of an oceanic area between the Anatolide-Tauride Block and the Kırşehir Block in Mesozoic period. Only limited data is available for the opening of this oceanic area, which is called the Inner Tauride Ocean and Görür et al. (1984) suggests Early Jurassic.

Field observations and geochemical/ geochronological data on the studied amphibolites indicate that initiation of the rifting in Anatolide-Tauride block, opening of the Inner Tauride Ocean and breaking-away processes of the Kırşehir Block occured during Middle-Late Triassic period in terms of long-term periodic extensional processes along the northern margin of the Gondwana. These new findings reveal that the Anatolide-Tauride Block and the Kırşehir Block were contemporaneously broken-away from the northern part of Gondwana.

Acknowledgements

This study was carried out within the scope of the project of tectono-stratigraphic characteristics of the Niğde Massif which was run by the Department of Geological Survey, General Directorate of Mineral Research and Exploration. The chemical analyzes of the samples from the metabasites cropping out in the study area were carried out at the Department of Mineral Analysis and Technology Laboratories (MTA), and the U-Pb geochronological studies were conducted at the University of Arizona, Department of Geosciences Laboratory (USA). Petrographic descriptions of the samples were defined by the geologists of Department of Geological Research: Ezgi ULUSOY, Aylin PAÇALA, Meral GÜREL and Yelda ILGAR.

References

Advokaat, E. L., Van Hinsbergen, D. J. J., Kaymakçı, N., Vissers, R. L. M., Hendriks, B. W. 2014. Late Cretaceous extension and Palaeogene rotation-related contraction in Central Anatolia recorded in the Ayhan-Büyükkişla basin. International Geology Review 56(15), 1813-1836.

Agrawal, S., Guevara, M., Verma, S. 2008. Tectonic discrimination of basic and ultrabasic volcanic rocks throughlog-transformed ratios of immobile trace elements. International Geology Review 50, 1057-1079.

Akal, C., Koralay, E., Candan, O., Oberhansli, R., Chen, F. 2011. Geodynamic Significance of the Early Triassic Karaburun Granitoid (Western Turkey) for the Opening History of Neo-Tethys. Turkish Journal of Earth Science 20, 255-271.

Akal, C., Candan O., Koralay E., Oberhansli R., Chen, F., Prelevic, D. 2012. Early Triassic potassic volcanism in the Afyon Zone of the Anatolides/ Turkey: implications for the rifting of the Neo-Tethys. International Journal of Earth Sciences 101, 177-194.

Akdoğan, R., Okay, A. I., Dunkl, I. 2019. Striking variation in the provenance of the Lower and Upper Cretaceous turbidites in the central Pontides (northern Turkey) related to the opening of the Black Sea. Tectonics 38, 1050-1069.

Altumi, M., Elicki, O., Linnemann, U., Hofmann, M., Sagawe, A. 2013. A U-Pb LA-ICP-MS detrital zircon ages from the Cambrian of Al Qarqaf Arch, central-western Libya: Provenance of the West Gondwanan sand sea at the dawn of the early Palaeozoic. Journal of African Earth Sciences 79 (2013) 74-97.

Alpaslan, M., Frei, R., Kurt, M. A., Boztuğ D., Temel, A., Göncüoğlu, G., Gül, M., Uçurum, A. 2006. Ulukışla havzasının evrimine petrolojik bir yaklaşım. 59. Türkiye Jeoloji Kurultayı, 20-24 Nisan 2006, Ankara, 46-47.

Anders, B., Reischmann, T., Kostopoulos, D., Lehnert, O., Matukov, D., Sergeev, S. 2007. Zircon geochronology of basement rocks from the Pelagonian Zone, Greece: constraints on the pre Alpine evolution of the western most Internal Hellenides. International Journal Earth Science 96, 639-661.

Atabey, E., Göncüoğlu, M. C., Turhan, N. 1990. 1/100000 ölçekli Açınsama Nitelikli Türkiye Jeoloji Haritaları Serisi, Kozan-J19 Paftası, No: 33. Maden Tetkik ve Arama Genel Müdürlüğü, Ankara.

Aydın, N. S., Göncüoğlu, M. C., Erler, A. 1998. Latest Cretaceous magmatism in the Central Anatolian crystalline complex: review of field, petrographic and geochemical features. Turkish Journal of Earth Sciences 7, 259-268.

Bailey, E. B., Mc Callien, W. J. 1950. Ankara melanjı ve Anadolu şariyajı. Bulletin of the Mineral Research and Exploration 15(40).

Barrier, E., Vrielynck, B., Brouillet, J. F., Brunet, M. F. 2018. Paleotectonic reconstruction of the Central Tethyan realm. tectonono-sedimentary-palinspastic maps from Late Permian to Pliocene. DARIUS project maps.

Baykal, E. 1947. Zile-Tokat-Yıldızeli bölgesinin jeolojisi. İstanbul Üniversitesi Fen Fakültesi Dergisi 12(3), B, 191-209.

Beyazpirinç, M., Akçay, A. E. 2017. Akdağmadeni Masifi'nin jeolojisi ve jeodinamik evrimi. Maden Tetkik ve Arama Genel Müdürlüğü, Rapor No: 13569, 166, Ankara (unpublished).

Beyazpirinç, M., Akçay, A. E., Özkan, M. K., Sönmez, M. K., Dönmez, M. 2020. Kırşehir Masifi'nin tektono-stratigrafik özellikleri. Maden Tetkik ve Arama Genel Müdürlüğü, Rapor No: 13934, 200, Ankara (unpublished).

Blumenthal, M. M. 1952. Das taurische hochgebirge des Aladağ, neuere forschungen zur seiner geographie, stratigraphie und tektonik. Maden Tetkik ve Arama Enstitüsü Yayın serisi 6, 136.

Boztuğ, D., Jonckheere, R. C., Heizler , M., Ratschbacher, L., Harlavan, Y., Tichomirova, M. 2009. Timing of post-obduction granitoids from intrusion through cooling to exhumation in central Anatolia, Turkey. Tectonophysics 473(1-2), 20, 223-233.

Boynton, W. V. 1984. Cosmochemistry of the rare earth elements; meteorite studies. Rare earth element geochemistry. Henderson, P. (Ed.). Elsevier, Amsterdam, 63-114.

Cabanis, B., Lecolle, M. 1989. Le diagramme La/10-Y/15-Nb/8: un outilpour la discrimination desséries volcaniques et la mise en évidencedes processus de mélange et/ou de contamination crustale. Comptesrendus de l'Académiedes sciences. Série 2, Mécanique, Physique, Chimie, Sciences de l'univers. Sciences de la Terre 309, 2023-2029.

Candan, O., Çetinkaplan, M., Oberhansli, R., Rimmele, G., Akal, C. 2005. Alpine high-pressure/low temperature metamorphism of Afyon Zone and implication for metamorphic evolution of western Anatolia, Turkey. Lithos 84, 102-124.

Candan, O., Akal, C., Koralay, O. E., Okay, A. I., Oberhänsli, R., Prelević, D., Mertz-Kraus, R. 2016. Carboniferous granites on the northern margin of Gondwana, Anatolide-Tauride Block, Turkey-Evidence for southward subduction of Paleotethys. Tectonophysics 683, 349-366.

Cengiz Çinku, M., Hisarli, Z. M., Yılmaz, Y., Ülker, B., Kaya, N., Öksüm, E., Orbay, N., Özbey, Z. Ü. 2016. The tectonic history of the Niğde-Kırşehir Massif and the Taurides since the Late Mesozoic: Paleomagnetic evidence for two-phase orogenic curvature in Central Anatolia. Tectonics 35, 772-811.

Clark, M., Robertson, A. H. F. 2002. The role of the Early Tertiary Ulukısla basin, Southern Turkey, in suturing of the Mesozoic Tethys Ocean. Journal of the Geological Society of London 159, 673-690.

Çemen, I., Göncüoğlu, M. C., Dirik, K. 1999. Structural evolution of the Tuzgölü basin in central Anatolia, Turkey. Journal of Geology 107, 693-706.

Çoban, M. 2019. Niğde Masifi'nin doğu kesiminin (Eynelli-Bademdere-Dikilitaş) jeolojisi ve yapısal özellikleri. Yüksek Lisans Tezi, Konya Teknik Üniversitesi, 133 (unpublished).

Dalkılıç, H. 2009. 1/100.000 ölçekli Türkiye Jeoloji Haritaları, No: 124. Maden Tetkik ve Arama Genel Müdürlüğü, Ankara.

Demircioğlu, R., Eren, Y. 2003. Niğde Masifi (Çamardı-Niğde) Tersiyer yaşlı örtü kayaçlarındaki Oligosen öncesi paleo-gerilme konumu. Süleyman Demirel Üniversitesi Mühendislik ve Mimarlık Fakültesi, 20. Yıl Jeoloji Sempozyumu, 37.

Demircioğlu, R., Eren, Y. 2017. Çamardı (Niğde) yöresinde Niğde Masifi'nin yapısal özellikleri. Bulletin of the Mineral Research and Exploration 154, 15-26.

Demircioğlu, R., Coşkuner, B. 2021. Gümüşler-Özyurt (Niğde) arasının yapısal özellikleri. Alanya Alattin Keykubat Üniversitesi Fen Bilimleri Dergisi 2(3), 120-12.

Dökmeci, İ. 1980. Akdağmadeni yöresinin jeolojisi. Maden Tetkik ve Arama Genel Müdürlüğü, Rapor No: 6953, Ankara (unpublished).

Egeran, E. N., Lahn, E. 1951. Kuzey ve Orta Anadolu'nun tektonik durumu hakkında not. Maden Tetkik ve Arama Dergisi 41, 23-27.

Engel, M., Reischmann, T. 1998. Single zircon geochronology of orthogneisses from Paros, Greece. Bulletin of the Geological Society of Greece 32 (3), 91-99.

Erkan, Y., Ataman, G. 1981. Orta Anadolu Masifi (Kırşehir yöresi) metamorfizma yaşı üzerine K-Ar yöntemi ile bir inceleme. Yerbilimleri Dergisi 8, 27-30.

Erler, A., Bayhan, H. 1995. Orta Anadolu granitoyitlerinin genel değerlendirilmesi ve sorunları. Yerbilimleri 17, 49-67.

Fedo, C. M., Sircombe, K. N., Rainbird, R. H. 2003. Detrital zircon analyses of the sedimentary record.

Hanchar, J. M., Hoskin, P. W. O. (Ed.). Zircon. Reviews in Mineralogy and Geochemistry 53, 277-303.

Gamkrelidze, I., Shengelia, D., Tsutsunava, T., Chung, S. L., Yichiu, H., Chikhelidze, K. 2011. New data on the U-Pb zircon age of the pre-alpine crystalline basement of the Black-Sea-Central Transcaucasian terrane and their geological significance. Bulletin of Georgian National Academy Science 5, 64-76.

Gessner, K., Collins, A. S., Ring, U., Güngör, T. 2004. Structural and thermal history of poly-orogenic basement: U-Pb geochronology of granitoid rocks in the southern Menderes Massif, Western Turkey. Journal of Geological Society 161, 93-101.

Göncüoğlu, M. C. 1977. Geologie des westlichen Niğde Massivs. Doktora Tezi, Bonn Tjniv University, 181 (unpublished).

Göncüoğlu, M. C. 1981. Niğde masifinin jeolojisi. İç Anadolu'nun Jeoloji Simpozyumu, Türkiye Jeoloji Kurumu Yayınları, 16-19.

Göncüoğlu, M. C., Toprak, V., Kuşcu, I., Erler, A., Olgun, E. 1991. Geology of the western part of the Central Anatolian Massif, part 1: southern section. Turkish Petroleum Corporation (TPAO), Report No: 2909, 1-140 (In Turkish).

Göncüoğlu, M. C., Erler, A., Toprak, V., Yalınız, K. M., Kuscu, I., Köksal, S., Dirik, K. 1993. Orta Anadolu Masifinin batı bölümünün jeolojisi. Bölüm 3: Orta Kızılırmak Tersiyer baseninin jeolojik evrimi. Turkish Petroleum Corporation (TPAO), Report No: 3313.

Göncüoğlu, M. C., Turhan, N., Tekin, U. K. 2003. Evidence for theTriassic rift ing and opening of the Neotethyan İzmir-Ankara Ocean, northern edge of the Tauride-Anatolide Platform, Turkey. Bulletin of Geological Society Italy 2, 203-212.

Göncüoğlu, M. C., Çapkınoğlu, Ş., Gürsu, S., Noble, P., Turhan, N., Tekin, U. K., Okuyucu, C., Göncüoğlu, Y. 2007. The Mississippian in the Central and Eastern Taurides (Turkey): constraints on the tectonic setting of the Tauride-Anatolide Platform. Geologica Carpathica 58, 427-442.

Görür, N., Oktay, F. Y., Seymen, İ., Şengör, A. M. C. 1984. Palaeotectonic evolution of the Tuzgölü basin complex, Central Turkey: sedimentary record of a Neo-Tethyan closure. Geological Society of London, Special Publications 17(1), 467-482.

Görür, N., Tüysüz, O., Şengör, A. M. C. 1998. Tectonic evolution of the Central Anatolian basins. International Geology Review 40, 831-850.

Johnson, P., Kattan F. 2007. Geochronologic dataset for precambrian rocks in the Arabian peninsula a catalogue of U-Pb, Rb-Sr, Ar-Ar, and Sm-Nd ages. Open-file Report No: SGS-OF-2007-3 1428 H 2007 G.

Johnson, P. R., Andresen, A., Collins, A. S., Fowler, A. R., Fritz, H., Ghebreab, W., Kusky, T., Stern, R. J. 2011. Late Cryogenian-Ediacaran history of the Arabian-Nubian Shield. A review of depositional, plutonic, structural, and tectonic events in the closing stages of the northern East African orogen. Journal of African Earth Sciences 61, 167-232.

Kara, H., Dönmez, M. 1990. 1/100000 ölçekli Açınsama Nitelikli Türkiye Jeoloji Haritaları Serisi, Kırşehir-G17 Paftası, No:34. Maden Tetkik ve Arama Genel Müdürlüğü, Ankara.

Ketin, İ. 1955. Yozgat bölgesinin jeolojisi ve Orta Anadolu masifinin tektonik durumu. Türkiye Jeoloji Kurumu Bülteni 6, 1-40.

Ketin, İ. 1963. 1/500 000 ölçekli Türkiye Jeoloji Haritası (Kayseri). Maden Tetkik ve Arama Genel Müdürlüğü Yayını, 82, Ankara.

Koralay, O. E., Satır, M., Dora, O. O. 2001. Geochemical and geochronological evidence for Early Triassic calc-alkaline magmatism in the Menderes Massif, western Turkey. International Journal of Earth Sciences 89, 822-835.

Le Bas, M. J., Le Maitre, R. W., Streckeisen, A., Zanettin, B. 1986. A chemical classification of volcanic rocks based on the total alkali-silica diagram. Journal of Petrology 27, 745-750.

Linnemann, U., Gerdes, A., Drost, K., Buschmann, B. 2007. The continuum between Cadomian orogenesis and opening of the Rheic Ocean: constraints from LA-ICP-MS U-Pb zircon dating and analysis of plate-tectonic setting (Saxo-Thuringian zone, northeastern Bohemian Massif, Germany). Geological Society of America, Special Paper 423, 61-96.

Löwen, K., Meinhold, G., Güngör, T., Berndt, J. 2017. Palaeotethys-related sediments of the Karaburun Peninsula, western Turkey: Constraints on provenance and stratigraphy from detrital zircon geochronology: International Journal of Earth Sciences 106(8), 2771-2796.

Löwen, K., Meinhold, G., Arslan, A., Güngör, T., Berndt, J. 2018. Evolution of the Palaeotethys in the Eastern Mediterranean: Age, provenance and tectonic setting of the Upper Palaeozoic Konya Complex and its Mesozoic cover sequence (south-central

Turkey), Geo Bonn 2018, Bonn, Germany, 2-6 September 2018, Abstracts, 61.

Löwen, K., Meinhold, G., Arslan, A., Güngör, T., Berndt, J. 2019. Evolution of the Paleotethys in the Eastern Mediterranean: a multi-method approach to unravel the age, provenance and tectonic setting of the Upper Paleozoic Konya Complex and its Mesozoic cover sequence (south-central Turkey). International Geology Review 62(4), 389-414.

Meinhold, G., Reischmann, T., Kostopoulos, D., Lehnert, O., Matukov, D., Sergeev, S. 2008. Provenance of sediments during subduction of Palaeotethys: Detrital zircon ages and olistolith analysis in Palaeozoic sediments from Chios Island, Greece. Palaeogeography, Palaeoclimatology, Palaeoecology 263, 71-1.

Monod, O., Kozlu, H., Ghienne, W., Dean, W.T., Günay, Y., Herisse, A., Paris, F. 2003. Late Ordovician glaciations in southern Turkey. Terra Nova 15(4), 249-257.

Muttoni, G., Kent, D. V., Garzanti, E., Brack, P., Abrahamsen, N., Gaetani, M. 2003. Early Permian Pangea B to Late Permian Pangea A. Earth and Planetary Science Letters 215, 379-394.

Okay, A. I., Tüysüz, O. 1999. Tethyan sutures of northern Turkey. Geological Society of London, Special Publications 156(1), 475-515.

Okay, A. I. 2000. Was the Late Triassic orogeny in Turkey caused by the collision of an oceanic plateau? Bozkurt, E., Winchester, J. A., Piper, J. A. D. (Ed.). Tectonics and magmatism in Turkey and surrounding area, Geological Society of London, Special Publication 173, 25-41.

Okay, A. I., Satır, M., Siebel, M. 2006. Pre-Alpide Palaeozoic and Mesozoic orogenic events in the Eastern Mediterranean region. Gee, D. G., Stephenson, R. A. (Ed.). European Lithosphere Dynamics. Geological Society of London, Memoirs 32, 389-405.

Okay, A. I., Satır, M., Shang, C. 2008. Ordovician metagranitoid from the Anatolide-Tauride Block, northwest Turkey: geodynamic implications. Terra Nova 20, 280-288.

Okay, N., Zack. T., Okay, A. I., Barth, M. 2011. Sinistral transport along the Trans-European Suture Zone: detrital zircon-rutile geochronology and sandstone petrography from the Carboniferous flysch of the Pontides. Geological Magazine 148(3), 380-403.

Okay, A. I., Nikishin, A. M. 2015. Tectonic evolution of the southern margin of Laurasia in the Black Sea region. International Geology Review 57(5-8).

Okay, A. I., Topuz, G. 2017. Variscan Orogeny in the Black Sea region. International Journal of Earth Sciences 106, 569-592.

Okay, A. I., Zattin, M., Özcan, E., Sunal, G. 2020. Uplift of Anatolia. Turkish Journal of Earth Sciences 29, 696-713.

Özdamar, Ş., Billor, M., Sunal, G., Esenli, F., Roden, M. 2013. First U-Pb SHRIMP zircon and 40Ar/39Ar ages of metarhyolites from the Afyon-Bolkardag Zone, SW Turkey: implications for the rifting and closure of the Neo-Tethys. Gondwana Research 24, 377-391.

Özgül, N. 1976. Torosların bazı temel jeolojik özellikleri. Türkiye Jeoloji Kurumu Bülteni 19, 65-78.

Özgül, N., Kozlu, H. 2002. Kozan-Feke (Doğu Toroslar) yöresinin stratigrafisi ve yapısal konumu ile ilgili bulgular. TPJD Bülteni 14(1), 1-36.

Parlak, O., Robertson, A. 2004. The ophiolite-related Mersin Melange, southern Turkey: its role in the tectonic-sedimentary setting of Tethys in the Eastern Mediterranean region. Geological Magazine 141 (3), 257-286.

Pearce, J. A. 1983. Role of the sub-continental lithosphere in magma genesis at destructive plate margins. Hawkeswoeth, C. J., Norry, M. J. (Ed.). Continental basalts and Mantle Xenolithes. Nantwich, Shiva, 230-249.

Pearce, J. A. 1996. A user's guide to basalt discrimination diagrams. Wyman, D. A. (Ed.) Trace Element geochemistry of volcanic rocks: applications for massive sulphide exploration. Geological Association of Canada, Short Course Notes 12, 79-113.

Pearce, J. A. 2008. Geochemical fingerprinting of oceanic basalts with applications to ophiolite classification and the search for Archean oceanic crust. Lithos 100, 14-48.

Perinçek, D. 1990. Hakkari ili ve dolayının stratigrafisi, GDA Türkiye. Türkiye Petrol Jeologları Derneği Bülteni 2, 21-68.

Phillipson, 1915. Reisen und forschungen im westlichen kleinasien. Pett, Mitt., H., 167.

Pourteau, A., Candan, O., Oberhänsli, R. 2010. High-pressure metasediments in central Turkey: constraints on the Neotethyan closure history. Tectonics 29.

Robertson, A. H. F., Ustaömer, T. 2009. Role of Upper Palaeozoic subduction/accretion processes in the closure of Palaeotethys: evidence from the Chios

Melange (E Greece), the Karaburun Melange (W Turkey) and the Teke Dere Unit, SW Turkey. Sedimentary Geology 220, 29-59.

Robertson, A., Parlak, O., Ustaömer, Y. 2021. Late Palaeozoic extensional volcanism along the northern margin of Gondwana in southern Turkey: implications for Palaeotethyan development. International Journal of Earth Sciences 110, 1961-1994.

Robinson, F., Foden, J. D., Collins Payne, A. S. J. L. 2014. Arabian Shield magmatic cycles and their relationship with Gondwana assembly: Insights from zircon U-Pb and Hf isotopes. Earth and Planetary Science Letters 408, 207-225.

Seymen, İ. 1981*a*. Kaman (Kırşehir) dolayında Kırşehir masifinin stratigrafisi ve metamorfizması. İç Anadolu'nun Jeoloji Simpozyumu, Türkiye Jeoloji Kurumu Bülteni 24(2), 7-14.

Seymen, İ. 1981*b*. Kaman (Kırşehir) dolayında Kırşehir masifinin metamorfizması. İç Anadolu'nun Jeoloji Simpozyumu, Türkiye Jeoloji Kurumu Bülteni, 24 (2), 101-108.

Seymen, İ. 1982. Kaman dolayında Kırşehir masifinin jeolojisi. Doçentlik Tezi, İstanbul Teknik Üniversitesi Maden Fakültesi, 164, İstanbul (unpublished).

Stampfli, G. M., Borel, G. D. 2002. A plate tectonic model for the Paleozoic and Mesozoic constrained by dynamic plate boundaries and restored synthetic oceanic isochrones. Earth and Planetary Science Letters 196, 17-33.

Stampfli, G. M., Hochard, C., Verard, C., Vilhem, C., Von Raumer, J. 2013. Formation of Pangea. Tectonophysics 593, 1-19.

Stern, R. J. 1994. Arc assembly and continental collusion in the Proterozoic east African orogen: implications for the consolidation of Gondwanaland. Annual Review of Earth Planet Sciences 22, 319-351.

Şahin, M. B. 1991. Basçatak köyü (Akdağmadeni-Yozgat) doğusunun jeolojik ve petrografik özelliklerinin incelenmesi. Yüksek Lisans Tezi, Hacettepe Üniversitesi Fen Bilimleri Enstitüsü, 68, Ankara (unpublished).

Şengör, A. M. C., Yılmaz, Y. 1981. Tethyan evolution of Turkey. A Plate Tectonic Approach. Tectonophysics 75, 181-241.

Şengör, A. M. C., Satır, M., Akkök, R. 1984. Timing of tectonic events in the Menderes Massif, western Turkey: implications for tectonic evolution and evidence for Pan-African basement in Turkey. Tectonics 3, 693-707.

Topuz, G., Altherr, R., Satır, M., Schwarz, M. 2004. Lowgrade metamorphic rocks from the Pulur complex, NE Turkey: implications for pre-Liassic evolution of the Eastern Pontides. International Journal of Earth Sciences 93, 72-91.

Topuz, G., Altherr, R., Schwartz, W.H., Dokuz, A., Meyer, H-P. 2007. Variscan amphibolites-facies rocks from the Kurtoğlu metamorphic complex (Gümüşhane area, Eastern Pontides, Turkey). International Journal of Earth Science 96, 861-873.

Topuz, G., Altherr, R., Siebel, W., Schwarz, W. H., Zack, T., Hasözbek, A., Barth, M., Satır, M., Cüneyt, Ş. 2010. Carboniferous highpotassium I-type granitoid magmatism in the Eastern Pontides: the Gümüşhane pluton (NE Turkey). Lithos 116, 92-110.

Topuz, G., Candan, O., Okay, A.I., Quadt, A., Othman, M., Zack, T., Wang, J. 2020. Silurian anorogenic basic and acidic magmatism in Northwest Turkey: implications for the opening of the Paleo-Tethys. Lithos 356-357, 105302.

Topuz, G., Candan, O., Wang, J., Li, Q., Wuc, F., Yılmaz, A. 2021. Silurian A-type metaquartz-syenite to-granite in the Eastern Anatolia: implications for Late Ordovician-Silurian rifting at the northern margin of Gondwana. Gondwana Research 911-17.

Torsvik, T. H., Cocks, L. R. M. 2013. Gondwana from top to basein space and time. Gondwana Research 24, 999-1030.

Ustaömer, P. A., Ustaömer, T., Collins, A. S., Robertson, A. H. F. 2009. Cadomian (Ediacaran-Cambrian) arc magmatism in the Bitlis Massif, SE Turkey: magmatism along the developing northern margin of Gondwana. Tectonophysics 473, 99-112.

Ustaömer, P. A., Ustaömer, T., Gerdes, A., Robertson, A. H. F., Collins, A. S. 2012. Evidence of Precambrian sedimentation/ magmatism and Cambrian metamorphism in the Bitlis Massif, SE Turkey utilising whole-rock geochemistry and U-Pb LA-ICP-MS zircon dating: Gondwana Research 21, 1001-1018.

Ustaömer, T., Robertson, A.H., Ustaömer, P.A., Gerdes, A., Peytcheva, I. 2013. Constraints on Variscan and Cimmerian magmatism and metamorphism in the Pontides (Yusufeli-Artvin area), NE Turkey from U-Pb dating and granite geochemistry. Geological Society of London, Special Publications 372 (1), 49-74.

Ustaömer, T., Ustaömer, P. A., Robertson, A. H., Gerdes, A. 2016. Implications of U-Pb and Lu-Hf isotopic analysis of detrital zircons for the depositional age, provenance and tectonic setting of the Permian-Triassic Palaeotethyan Karakaya complex, NW Turkey. International Journal of Earth Sciences 105(1), 7-38.

Ustaömer, T., Ustaömer, P., Robertson, A., Gerdes, A. 2019. U-Pb-Hf isotopic data from detrital zircons in late Carboniferous and Mid-Late Triassic sandstones, and also Carboniferous granites from the Tauride and Anatolide continental units in S Turkey: implications for Tethyan Palaeogeography. Internatıonal Geology Review 62 (9).

Von Raumer J. F., Stampfli, G. M. 2008. The birth of the Rheic Ocean-Early Palaeozoic subsidence patterns and subsequenttectonic plate scenarios. Tectonophysics 461, 9-20.

Winchester, J. A., Park, R. G., Holland, J. G. 1980. The geochemistry of Lewisian semipelitic schists from the Gairloch District, Wester Ross. Scottish Journal of Geology 16, 165-79.

Winchester, J. A., Max, M. D. 1982. The geochemistry andorigins of the Precambrian rocks of the Rosslare Complex, S. E. Ireland. Journal of Geological Society of London 139, 309-19.

Whitney, D. L., Teyssier, C., Dilek, Y., Fayon, A. K. 2001. Metamorphism of the central anatolian crystalline complex, Turkey: influence of orogen-normal collision vs wrench-dominated tectonics on P-T-t paths. Journal of Metamorphic Geology 19, 411-432.

Whitney, D. L., Teyssier, C., Heizler, M. T. 2007. Gneiss domes, metamorphic core complexes, and wrench zones: thermal and structural evolution of the Niğde massif central Anatolia. Tectonics 26, 1-23.

Yalınız, K. M., Göncüoglu, M. C. 1998. General geological characteristics and distribution of the Central Anatolian Ophiolites. Yerbilimleri 20, 19-30.

Zhou, M. F., Lesher, C. M., Yang, Z., Li, J. W., Sun, M. 2004. Geochemistry and petrogenesis of 270 Ma Ni-Cu-(PGE) sulfidebearing mafic intrusions in the Huangshan district, Eastern Xinjiang, Northwest China: implications for the tectonic evolution of the Central Asian orogenic belt. Chemical Geology 209(3-4), 233-257.

Zlatkin, O., Avigad, D., Gerdes, A. 2013. Evolution and provenance of Neoproterozoic basement and lower Paleozoic siliciclastic cover of the Menderes Massif (western Taurides): coupled U-Pb-Hf zircon isotope geochemistry: Gondwana Research 23, 682-700.